NAVAL POSTGRADUATE SCHOOL
Monterey, California

THESIS

STRUCTURAL PROPERTY EFFECTS
FOR PLATINUM MODIFIED ALUMINIDE COATINGS

by

LCDR Lawrence G. Newman

September 1986

Thesis Advisor: Dr. D.H. Boone

Approved for public release; distribution unlimited.

URITY CLASSIFICATION OF THIS PAGE

REPORT DOCUMENTATION PAGE

REPORT SECURITY CLASSIFICATION Unclassified	1b. RESTRICTIVE MARKINGS
SECURITY CLASSIFICATION AUTHORITY	3. DISTRIBUTION / AVAILABILITY OF REPORT Approved for public release; distribution unlimited.
DECLASSIFICATION / DOWNGRADING SCHEDULE	
PERFORMING ORGANIZATION REPORT NUMBER(S)	5 MONITORING ORGANIZATION REPORT NUMBER(S)
NAME OF PERFORMING ORGANIZATION Naval Postgraduate School 6b OFFICE SYMBOL (If applicable) 69	7a. NAME OF MONITORING ORGANIZATION Naval Postgraduate School
ADDRESS (City, State, and ZIP Code) Monterey, California 93943-5000	7b. ADDRESS (City, State, and ZIP Code) Monterey, California 93943-5000
NAME OF FUNDING / SPONSORING ORGANIZATION 8b. OFFICE SYMBOL (If applicable)	9. PROCUREMENT INSTRUMENT IDENTIFICATION NUMBER
ADDRESS (City, State, and ZIP Code)	10 SOURCE OF FUNDING NUMBERS PROGRAM ELEMENT NO. / PROJECT NO / TASK NO. / WORK UNIT ACCESSION NO

TITLE (Include Security Classification)

STRUCTURAL PROPERTY EFFECTS FOR PLATINUM MODIFIED ALUMINIDE COATINGS

PERSONAL AUTHOR(S)
Newman, Lawrence G.

a TYPE OF REPORT	13b TIME COVERED	14 DATE OF REPORT (Year, Month, Day)	15 PAGE COUNT
Master's Thesis	FROM _____ TO _____	1986 September	57

SUPPLEMENTARY NOTATION

COSATI CODES			18 SUBJECT TERMS (Continue on reverse if necessary and identify by block number)
FIELD	GROUP	SUB-GROUP	Coatings, Aluminide Coatings, DBTT, Diffusion Aluminide Coatings, Platinum Modified Aluminide Coatings

) ABSTRACT (Continue on reverse if necessary and identify by block number)

Aluminide and platinum modified aluminide coatings have proven to be effective and economical means of protecting gas turbine components from oxidative and corrosive attack. In order to maintain coating integrity, the response of the coating-substrate system to strains imposed by thermal expansion mismatch and external stresses must be known. Selected coating systems were examined on an IN 738 substrate to determine the ductile to brittle transition temperature (DBTT) and the residual strains caused by the presence of the coating. The coating morphology was examined by scanning electron microscopy and electron probe microanalysis, and correlations between coating microstructure and DBTT were established.

0 DISTRIBUTION / AVAILABILITY OF ABSTRACT ☒ UNCLASSIFIED/UNLIMITED ☐ SAME AS RPT ☐ DTIC USERS	21. ABSTRACT SECURITY CLASSIFICATION Unclassified
2a NAME OF RESPONSIBLE INDIVIDUAL Dr. D.H. Boone	22b TELEPHONE (Include Area Code) (408) 646-2586 22c. OFFICE SYMBOL 69B1

D FORM 1473, 84 MAR 83 APR edition may be used until exhausted
All other editions are obsolete

SECURITY CLASSIFICATION OF THIS PAGE

Approved for public release; distribution is unlimited.

Structural Property Effects for Platinum Modified Aluminide Coatings

by

Lawrence G. Newman
Lieutenant Commander, United States Navy
B.S., Auburn University, 1975

Submitted in partial fulfillment of the
requirements for the degree of

MASTER OF SCIENCE IN MECHANICAL ENGINEERING

from the

NAVAL POSTGRADUATE SCHOOL
September 1986

ABSTRACT

Aluminide and platinum modified aluminide coatings have proven to be effective and economical means of protecting gas turbine components from oxidative and corrosive attack. In order to maintain coating integrity, the response of the coating - substrate system to strains imposed by thermal expansion mismatch and external stresses must be known. Selected coating systems were examined on an IN 738 substrate to determine the ductile to brittle transition temperature (DBTT) and the residual strains caused by the presence of the coating. The coating morphology was examined by scanning electron microscopy and electron probe microanalysis, and correlations between coating microstructure and DBTT were established.

TABLE OF CONTENTS

LIST OF TABLES

LIST OF FIGURES

ACKNOWLEDGEMENTS

The advice and patience of Dr. D.H. Boone and the technical support of Mr. Colin Thomas of Howmet Corporation and Dr. S. Shankar of Turbine Components Corporation are gratefully acknowledged.

I. INTRODUCTION

The gas turbine as a useful power and propulsion plant is a fairly recent development, although the concept is several centuries old. The earliest gas turbine patent was issued to John Barber in 1791, but the first commercial gas turbine engines were not developed until the late 1930's and early 1940's [Ref. 1:pp. 24-27]. The first United States Navy contract for a gas turbine power plant was awarded to Allis - Chalmers in 1940, and by the 1950's gas turbines were in use as propulsion plants in minesweeping boats and some landing craft and as power generation units in several destroyers and cruisers [Ref. 2].

The early turbines were plagued by mechanical failures and low efficiencies and were constrained by the materials then in use. In 1941, the Henry Wiggin Company produced the first in the Nimonic alloy series, a nickel-chromium-cobalt precursor to today's superalloys, which was the first of many steps in developing alloys to improve gas turbine performance [Ref. 1:p. 29].

The rapid development in the forty years since WWII can be attributed to one major factor -- increased turbine inlet temperature. Efforts to produce materials with appropriate high temperature mechanical properties and to improve the cooling of surfaces in the hot gas stream have allowed these advances. Current turbine inlet temperatures are in the range of 2100°F for long life industrial gas turbines [Ref. 3] and 2500°F for advanced aircraft turbines [Ref. 1:p. 47]. The steady upwards trend in inlet temperatures is of continuing interest allowing designers to minimize power to weight ratios and to increase efficiencies.

The life limiting components of many gas turbines are the first stage blades. In addition to the high temperatures already noted, stresses in the range of 20,000 psi are typical [Ref. 4:p. 284]. The aggressive operating environment caused by the oxidizing hot gas stream results in a corrosion problem that limits first stage component life, and the problem is further aggravated by operation in the marine environment and use of poor quality fuels.

Early alloy development was targeted at increased creep strength and inherent corrosion resistance, but the operating conditons have become so severe that alloys developed for optimal strength, ductility, creep resistance and fatigue resistance do not

have sufficent corrosion capability. The last thirty years have seen the extensive development of coating systems to deal with this problem.

Previous work at the Naval Postgraduate School had validated an experimental procedure to determine ductile to brittle transition temperatures (DBTT) for coatings, collected low temperature data for selected platinum modified aluminide coatings and noted residual compressive strains in some of the coating systems. This research was designed to:

- Collect high temperature DBTT data.
- Measure residual coating strains.
- Determine DBTT for baseline aluminides without platinum.
- Establish coating structures and correlate with the DBTT.

II. HIGH TEMPERATURE CORROSION

A. BACKGROUND

The interaction of uncoated superalloy gas turbine components with the oxidizing hot gas stream has extremely deleterious effects. The problem is aggravated by contaminants which come from the fuel and intake air. Petroleum fuels have small but significant amounts of non- hydrocarbon constituents, principally sulfur, sodium, nitrogen, vanadium, nickel, iron and copper. For marine gas turbines, the ingested air contains a significant amount of sodium chloride and other sea water related impurities which further aggravates the corrosion problem. [Ref. 5:p. 51].

The interaction of the hot gases and the contaminants with the alloy substrate results in a depletion of the alloying elements, thereby decreasing the strength of the substrate. Roughened surfaces due to corrosion decrease the aerodynamic efficiency of rotating parts, and metal wastage may destroy or clog the fine cooling passages in complex turbine blades.

B. OXIDATION

Metals exposed to oxygen will react to form metallic oxides. The equilibrium reaction is determined by the Gibbs free energy of the resultant oxide and the partial pressure of the oxygen. For the operating conditions encountered in gas turbines, formation of the oxide scale is thermodynamically favorable for all but the precious metals.

Selective oxidation occurs in an alloy with the oxide that is most thermodynamically stable eventually forming, although reaction kinetics may dictate initial formation of a less stable oxide. Oxygen will continue to diffuse into the substrate and alloying elements will diffuse out. In the most fortituous case, the thermodynamically stable oxide scale will produce a dense, adherent and impervious layer and further substrate consumption is minimized.

As the existing oxide scale is cracked and spalled, unattacked substrate is exposed and more oxides form. The substrate gradually becomes depleted of the element being selectively oxidized and a less stable oxide forms as the degradation sequence continues. Al_2O_3 and Cr_2O_3 both form thermodynamically stable and effective barriers against further oxidation, with the aluminum oxide being more effective. Cr_2O_3 is not

used at temperatures above 1000°C as it reaches an equilibrium with gaseous CrO_3 [Ref. 6:pp. 2-15].

C. HOT CORROSION

Hot corrosion is a gas induced degradation modified by deposits on the oxide scale. The hot salts formed by the previously mentioned contaminants result in a fluxing reaction with the deposit, which is molten at these temperatures, reacting to dissolve the oxide scale. The major contaminants contributing to hot corrosion are vanadium, sodium and sulfur, which form V_2O_5 and Na_2SO_4. Molybdenum can also play a role if present, forming MoO_3. [Ref. 6:p. 19] The presence of NaCl accelerates the process of hot corrosion for some alloys [Ref. 7].

Hot corrosion may take place under either oxidizing or reducing conditions. The chemical reactions have been postulated but are quite complex [Ref. 8].

The reaction with Na_2SO_4 is the best documented and has been given the name sulfidation, although this really describes the reactions which occur in the substrate after the protective oxide has been breached. The alkali salt condenses on the hot turbine components and the oxide ions in the melt react with the scale. The protective scale is removed and the oxide ions prevent its regeneration. [Ref. 9:pp. 92-93] Continued degradation of the substrate occurs since a stable oxide barrier is not maintained.

III. THE SUPERALLOYS

A. GENERAL PROPERTIES

The superalloys are the nickel, cobalt and iron-nickel based families of alloys developed for use at high temperatures. Compositional and morphological control results in a wide range of alloys that are corrosion resistant and have excellent strength, creep resistance and ductility at severe operating temperatures [Ref. 10:p. 112]. The superalloys may be processed by the traditional deformation methods (forging or rolling), by casting (including investment casting), or by powder processing. Thermal expansion and thermal conductivity are relatively low [Ref. 11:pp. 16.7-16.10]. Processing to develop directional grain or crystal orientation is often used to take advantage of isotropic effects, and single crystal production is possible. Since grain boundaries are eliminated in single crystal parts, the alloying elements added as grain boundary strengtheners (carbon, boron, zirconium and hafnium) can be deleted, which allows development of alloys with higher melting temperatures, more homogeneous γ' distribution, and significantly greater strengths and fatigue resistances [Ref. 12:pp. 6-12].

B. THE NICKEL BASED SUPERALLOYS

The nickel based superalloys are characterized by an austenitic (face centered cubic) matrix phase, referred to as the γ phase, and a variety of second phases. The principal strengthening mechanisms are precipitation hardening and solid solution strengthening.

The common second phases are γ' and various carbides, most notably MC, $M_{23}C_6$, and M_6C. The γ' is the major contributor to precipitation hardening and is an ordered face centered cubic Ni_3Al intermetallic compound coherent with the matrix. [Ref. 13:p. 4].

IN 738 was the alloy selected as a substrate for this research. Its nominal compositon is listed in Table 1. The alloy is used extensively for turbine airfoils because of its strength, inherent corrosion resistance and adaptability to forming the complex castings required for modern turbine blades. For uses at temperatures above 1500°F, coatings are generally applied to prolong IN 738 component life. [Ref. 13:pp. 42-43.]

IV. COATING REQUIREMENTS AND PROCEDURES

A. REQUIREMENTS

The role of the protective aluminide coatings on superalloys is to provide a sufficient source of Al to form the Al_2O_3 scale. With the aluminum coming from the coating rather than from depletion of the substrate alloy, mechanical properties of the substrate can be maintained and the rich aluminum source allows replenishment of the stable and protective oxide scale.

In addition to corrosion protection, there are other requirements for the coating to be useful in practical applications. Some of the more important ones are [Refs. 14,15]:

- Erosion and impact resistance
- Thermal stability
- Adhesion
- Minimal influence on base alloy
- Economical application
- Adequate ductility

Erosion resistance is required to prevent coating destruction by particles entrained in the gas flow. If a coating is abraded or pitted by erosion, it can rapidly lose its corrosion resistance.

Coatings must be thermodynamically stable over the range of operating conditions encountered. If they undergo a phase change or rapidly diffuse into the substrate, they lose their effectiveness and may even degrade the base alloy properties.

Good adhesion is required to maintain the oxide barrier. Flaking or spalling under thermal and mechanical stresses at the blade surface lead to premature coating and component failure.

Mechanical properties of the base alloy can be significantly altered by coatings. The intrinsic heat treatment schedule peculiar to a given coating process, for example, can coarsen the γ' precipitate in precipitation strengthened superalloys and severely reduce creep and tensile strengths.

Adequate ductility to prevent coating cracking is another requirement. Ductility is important in maintaining coating integrity, but coating cracking due to inadequate

ductility can have a even more detrimental affect than loss of corrosion resistance. The coating cracks serve as initiation sites for fatigue and can lead to early and catastrophic component failure.

B. DUCTILE TO BRITTLE TRANSITION TEMPERATURE

The temperature at which a change from a low energy fracture to a high energy one occurs is called the DBTT. Transition temperatures are exhibited by body centered cubic and hexagonal close packed structures; above this temperature a material has the capacity to undergo extensive plastic deformation prior to failure [Ref. 16].

The nickel based superalloys have a face centered cubic structure and do not show marked variations in energy absorbed to failure as a function of temperature. The diffusion aluminide coatings based on the cubic NiAl do have a transition temperature, and if a coating does not have sufficient ductility at ambient temperatures it may still be suitable for use if the operating envelope of the turbine is above the DBTT for the coating.

C. COATING PROCESSES

There are several different methods used to apply protective coatings which have been well reviewed elsewhere [Refs. 17,18,19:pp. 177-186,79-116,121-136]. The one most commonly employed for diffusion aluminide coatings is the pack cementation process. This consists of arranging parts to be coated in a pack of aluminum rich metallic powder and refractory oxide filler. A halide is added to aid in transport of aluminum to the component surface. The entire pack is subjected to a heat treatment and the coating is formed by diffusion processes. The aluminum activity in the pack may be modified by changing the ratio of the powdered pack constituents, allowing aluminum levels in the coatings formed to be adjusted. [Ref. 20:pp. 50-53]

The morphology and composition of a coating are functions of the pack aluminum activity, the temperature at which the aluminizing process is conducted and the composition of the base alloy.

D. DIFFUSION ALUMINIDE COATINGS

The pack cementation process used to apply the diffusion aluminde coatings results in two structural types. Coatings applied at low temperatures and high aluminum activity (LTHA) are formed predominately by inward diffusion of aluminum from the surface and a three zone structure typically forms. The outermost zone is a δ

phase (Ni_2Al_3) and the inner zones are an aluminum rich β (NiAl) and a nickel rich β. Coatings applied at high temperatures and low aluminum activity (HTLA) are formed by outward nickel diffusion from the substrate and a two zone structure typically results. The external zone is an aluminum rich β phase and the internal zone is a nickel rich β. Both types of coatings exhibit an interdiffusion zone adjacent to the substrate formed by precipitation of supersaturated phases of the alloying elements as the nickel is depleted in this region. The morphology of the various layers can be changed by adjusting aluminum activity, temperature and post-coating heat treatment. [Refs. 21,22]

E. PLATINUM MODIFIED COATINGS

The addition of platinum to a diffusion aluminide coating has been shown to have beneficial results in certain types of corrosive environments [Refs. 23,24,25]. From a structural and mechanical properties standpoint it has two important considerations. The DBTT increases and an additional zone in the coating may form.

Platinum is electrodeposited on the substrate and a pre-aluminizing heat treatment is conducted. The coating morphology is dependent on the thickness of the platinum layer, the pre-aluminizing diffusion treatment and the coating process. Three platinum structures have been observed based on these variables [Refs. 26,27]:

- a continuous Pt_2Al_3 layer at the surface.
- $PtAl_2$ in a high Al β(NiAl) matrix.
- Pt in solution in the β(NiAl) phase.

V. EXPERIMENTAL PROCEDURE

A. SAMPLE SPECIMEN PREPARATION

The tensile specimens used were cast to shape from a commercial nickel based superalloy, IN 738. The castings were machined to net shape to conform to ASTM standards. The maximum specimen runout was held to less than 0.005 inches throughout the gage length to preclude development of bending stresses and to assure uniaxial specimen loading. [Ref. 28]

All specimens were ground to an 8-12 microinch RMS finish on the gage length to provide a consistent surface for subsequent coating treatments. The final gage diameter varied slightly from sample to sample due to the requirement to remove casting porosities and maintain a polished surface. Grooves were machined on the specimen shoulders to allow attachment of an extensometer.

Coatings were applied at two different commercial facilities using the aluminizing processes previously discussed. For the platinum modifed coatings, a 10 μm layer of platinum was electroplated directly on the gage length followed by selected heat treatments to diffuse the platinum into the specimen substrate. LTHA or HTLA aluminizing treatments and a heat treatment to restore substrate mechanical properties were conducted on all samples. Details of the coating and heat treatment schedules are listed in Table II. For the coating structural types selected, there are a number of variables in the coating process which can result in structural differences. These include aluminum level, platinum level and overall coating thickness, and some (e.g., aluminum level and coating thickness) are interrelated. The coating process parameters were selected to produce a nominal coating thickness of 75 μm, but for a constant aluminum pickup of 10-12 mg/cm^2, a variation in resultant thicknesses resulted for the various structures.

Each coating system selected for examination was applied to 4 tensile specimens and one control specimen. The DBTT data points and residual strains were measured using the tensile specimens, and structure morphology was examined using both sectioned tensile specimens and the control specimen.

B. TEST APPARATUS

A strain to coating failure method was used to determine the DBTT of each coating group. Tensile specimens were loaded at varying temperatures on a model TT-D Instron Universal Testing Instrument using a constant crosshead speed of 0.01 inches per minute. This resulted in a nearly constant strain rate of 1.2×10^{-4}.

A model 2232 Marshall clamshell furnace was used to control temperature. The furnace had a five inch temperature controlled zone maintained by three heating elements. Each element was controlled by an Omega model 48 controller.

Tensile specimens were mounted in an Applied Test Systems Series 4112 extensometer which allowed measurement of sample elongation using a dial gage while the specimen was at test temperature.

A type K chromel-alumel thermocouple was attached to the extensometer to be coincident with the center of the specimen under test. Digital temperature readouts were continously displayed with an accuracy of $\pm$ 1° C.

A dial gage with an accuracy of $\pm$ 0.0001 inch was attached to the extensometer below the furnace.

The lower pullrod of the extensometer was used as a wave guide for a Dunegan model S-140B transducer, which served as an input to a Textronix type 551 dual beam oscilloscope. Coating failure was acoustically monitored and visually observed on the oscilloscope trace. This procedure was adapted from a method previously used at NPS. [Refs. 29,30,31:p. 27]

Acoustical monitoring of coating cracking allows in situ study of crack formation. The acoustic emissions are characteristic of the irreversible process that generates the emissions [Ref. 32].

A Cambridge Stereoscan 200 Scanning Electron Microscope (SEM) was used at an acceleration voltage of 25 kV for structural studies.

A diagram of the test apparatus is included as Figure B.1.

C. TEST PROCEDURE

Test specimens were loaded at selected temperatures using a constant crosshead speed. The specimens were allowed to equilibrate for at least 15 minutes at the test temperature prior to straining.

Because the test specimens and the extensometer both exhibited a positive coefficient of thermal expansion, it was necessary to allow the apparatus to reach

equilibrium prior to inserting the lower crosshead pin in the testing machine to avoid putting the test rig under a compressive stress. Thermal gradients within the specimen were also avoided by this process.

The dial gage was zeroed at the test temperature so that only strain due to the applied load was measured. A tensile load was applied until coating cracking was indicated on the oscilloscope display. The elongation at coating failure was noted and the strain at coating failure was calculated. Sufficient calibration runs were made to establish the accuracy, sensitivity and repeatability of the procedure.

For comparison of test results the transition temperature was defined as that temperature which corresponded to a strain to coating failure of 0.6%, as previously suggested by Lowrie and Boone [Ref. 33].

Room temperature residual strains were measured using a plastic replication technique. A specimen which had been previously tested to coating failure but showed no crack opening because of residual stress was incrementally loaded at room temperature and replicas were taken. The replicas were examined using an optical microscope to determine when the cracks opened up, which was assumed to be the zero strain point in the coating. All specimens were remeasured to insure no plastic deformation had occured prior to residual strain measurement.

One specimen from each group was sectioned perpendicular to the tensile direction for coating structural studies. Selected plastically deformed specimens were sectioned parallel to the tensile direction to examine the crack morphology. The sectioned specimens were mounted and examined without etching.

The mounted and polished specimens were flashed with a gold film prior to SEM examination. Both the secondary electron emission and back scatter modes of the SEM were used. Elemental distribution within the coating was determined by conducting Electron Probe Micro Analysis (EPMA) at 2 μm intervals on the same mounts.

VI. RESULTS

A. STRUCTURES AND TRANSITION TEMPERATURES

Coating 1, an LTHA coating with minimal platinum pre-diffusion, formed a 100 μm coating with a continous $PtAl_2$ phase at the surface and did not exhibit a transition temperature over the range tested (see Figures B.2, B.3 and B.4). The platinum level remained constant over the initial 25 μm and then rapidly decreased.

Coating 2, an HTLA coating with medium platinum diffusion, formed a 75 μm coating with a single phase structure and a DBTT of 720°C (see Figures B.5, B.6 and B.7). The large spikes in the elemental distribution curve are caused by taking electron probe data near porosites or precipitates.

Coating 3, an LTHA coating with medium platinum diffusion, formed an 86 μm coating with a DBTT of 880°C (see Figures B.8, B.9 and B.10). The platinum was concentrated in the external third of the coating as dispersed $PtAl_2$ in a β phase matrix.

Coating 4, an HTLA coating with medium platinum diffusion, formed a 67 μm thick single phase coating with a DBTT of 750°C (see Figures B.11, B.12 and B.13). Superposition of figures B.6 and B.12 shows that the minor differences in the prealuminizing platinum diffusion did not change the platinum distribution significantly. The coatings show similar structures and DBTT's.

Coating 5, an HTLA coating with maximum platinum diffusion, formed a 130 μm thick coating and had a DBTT of 640°C (see Figures B.14, B.15 and B.16). The Pt was dispersed as a second phase in a β matrix.

Coating 6, the baseline LTHA coating, formed a typical inward 80 μm coating with a DBTT of 550°C (see Figures B.17, B.18 and B.19). As indicated in Table III, the room temperature strain to cracking was nearly 0.6% for this coating group which may lead to an artificially low value for the DBTT. An alternative method for defining the DBTT is by constructing tangents to both the low and high energy strain to coating failure curves and defining their intersection as the DBTT. For all coatings except this one both methods showed relatively good agreement; but for this coating the tangent-intercept method yielded a DBTT of 690°C.

Coating 7, the baseline HTLA coating, formed the characteristic two zone outward coating with a thickness of 55 μm and a DBTT of 580°C (see Figures B.20, B.21 and B.22).

Some of the DBTT data is based on curves generated from a few widely seperated points and the actual value obtained for the DBTT is dependent on the curve fitting technique. Comparison with the transition temperature data reported by Goward for the baseline aluminides is consistent, however detailed structural analyses are not available [Ref. 34].

Comparison of the coatings shows that aluminum levels, platinum distributions, coating thicknesses and coating morphologies can be varied and controlled by the processing parameters. The result is that an envelope of transition temperatures are obtained based on these variables. Coatings with higher surface Pt and Al levels exhibited higher DBTT's, and for the same pre-aluminizing Pt diffusion the HTLA process gave a lower DBTT. DBTT's are highest for the structures with a continuous $PtAl_2$ surface zone, and are minimized when the brittle $PtAl_2$ phase is dispersed in a NiAl matrix. However further reductions in Al levels allowing Pt to go into solution in NiAl (dissolution of the $PtAl_2$ phase) results in an apparent increase in the DBTT. The ductile to brittle transition temperatures are tabulated in Table IV.

B. RESIDUAL STRAIN

Figures B.23 and B.24 show typical coating cracks in section. As noted in Chapter V, these cracks were not visible at room temperature as a result of residual compressive stresses unless the sample had been plastically deformed. Use of plastic replicas allowed examination of a surface under load so that residual strains could be determined. Figure B.25 shows a plastically deformed cracked coating surface and Figure B.26 shows a replica of the surface for comparison purposes.

Residual strain results are tabulated in Table V. The baseline LTHA coating showed no residual strain; the baseline HTLA coating showed very low levels of compressive residual strains. However addition of platinum to the coating significantly increased residual compressive strains for all structures. Although the evidence is not conclusive because of the limited data available, it appears that $PtAl_2$ as a dispersed second phase in an NiAl matrix may minimize residual strain.

VII. CONCLUSIONS

The following conclusions can be drawn based on the results of this testing program:

- Pt modification increases the DBTT of an aluminide coating.
- A continuous $PtAl_2$ phase has the most severe effect on transition temperature.
- $PtAl_2$ as a dispersed second phase in an NiAl matrix is the optimum structure to minimize DBTT.
- Pt in solution in a low Al NiAl gives intermediate transition temperatures.
- Pt causes compressive residual strains in the diffusion aluminide coatings at room temperature.There may be some structural effect.
- Because there are so many interdependent variables in forming a diffusion aluminide coating, mechanical testing must be closely allied with structural characterization.

APPENDIX A
TABLES

TABLE I
IN 738 COMPOSITION

Element	Weight Percent
Ni	60.42
Cr	16.00
Co	8.50
Mo	1.75
W	2.60
Ti	3.40
Al	3.40
Nb	0.90
Ta	1.75
C	0.17
B	0.01
Zr	0.10
Fe	0.50 (max)
Mn	0.20 (max)
Si	0.30 (max)

TABLE II

COATINGS AND HEAT TREATMENTS

Coating Group	Coating and Heat Treatment
1	10 µm Pt electroplated 870 C / 0.5h LTHA aluminizing 1120 C / 2h 850 C / 24h
2	10 µm Pt electroplated 980 C / 2h HTLA aluminizing 1052 C / 4h 1120 C / 2h 850 C / 24h
3	10 µm Pt electroplated 1052 C / 1h LTHA aluminizing 1120 C / 2h 850 C / 24h
4	10 µm Pt electroplated 1052 C / 4h HTLA aluminizing 1052 C / 4h 1120 C / 2h 850 C / 24h
5	10 µm Pt electroplated 1080 C / 4h HTLA aluminizing 1052 C / 4h 1120 C / 2h 850 C / 24h
6	No Pt LTHA aluminizing 1120 C / 2h 850 C / 24h
7	No Pt HTLA aluminizing 1052 C / 4h 1120 C / 2h 850 C / 24h 850 C / 24h

TABLE III

STRAIN TO COATING CRACKING

Coating	Specimen	Test Temp. (C)	%Strain to Cracking
1	1*	21	0.36
	2*	810	0.36
	3	916	0.24
	4	20	0.27
2	1*	860	> 0.60
	2*	21	0.50
	3*	660	0.50
	4*	750	0.61
3	1*	810	0.25
	2*	21	0.28
	3*	300	0.28
	4*	550	0.25
	5	20	0.24
	6	934	1.19
4	1*	800	0.66
	2*	21	0.45
	3*	610	0.45
	4*	660	0.45
	5	20	0.20
5	1*	670	0.60
	2*	21	0.25
	3	560	0.40
6	1	600	> 0.63
	2	32	0.59
	3	780	0.97
	4	830	1.06
	5	933	> 3.30
7	1	20	0.48
	2	774	1.15
	3	23	0.41

Note: asterisked data points are from Reference 31, p. 44.

TABLE IV

DUCTILE TO BRITTLE TRANSITION TEMPERATURES

Platinum Diffusion	LTHA	HTLA
No Pt	550 C	580 C
870 C/0.5h	> 916 C	
980 C/2h		720 C
1052 C/1h	880 C	750 C
1080 C/4h		640 C

TABLE V

COMPRESSIVE RESIDUAL STRAINS

Platinum Diffusion	LTHA	HTLA
No Pt	0.00%	0.03%
870 C/0.5h	0.10%	
870 C/2h		0.16%
1052 C/1h	0.10%	0.12%

APPENDIX B

FIGURES

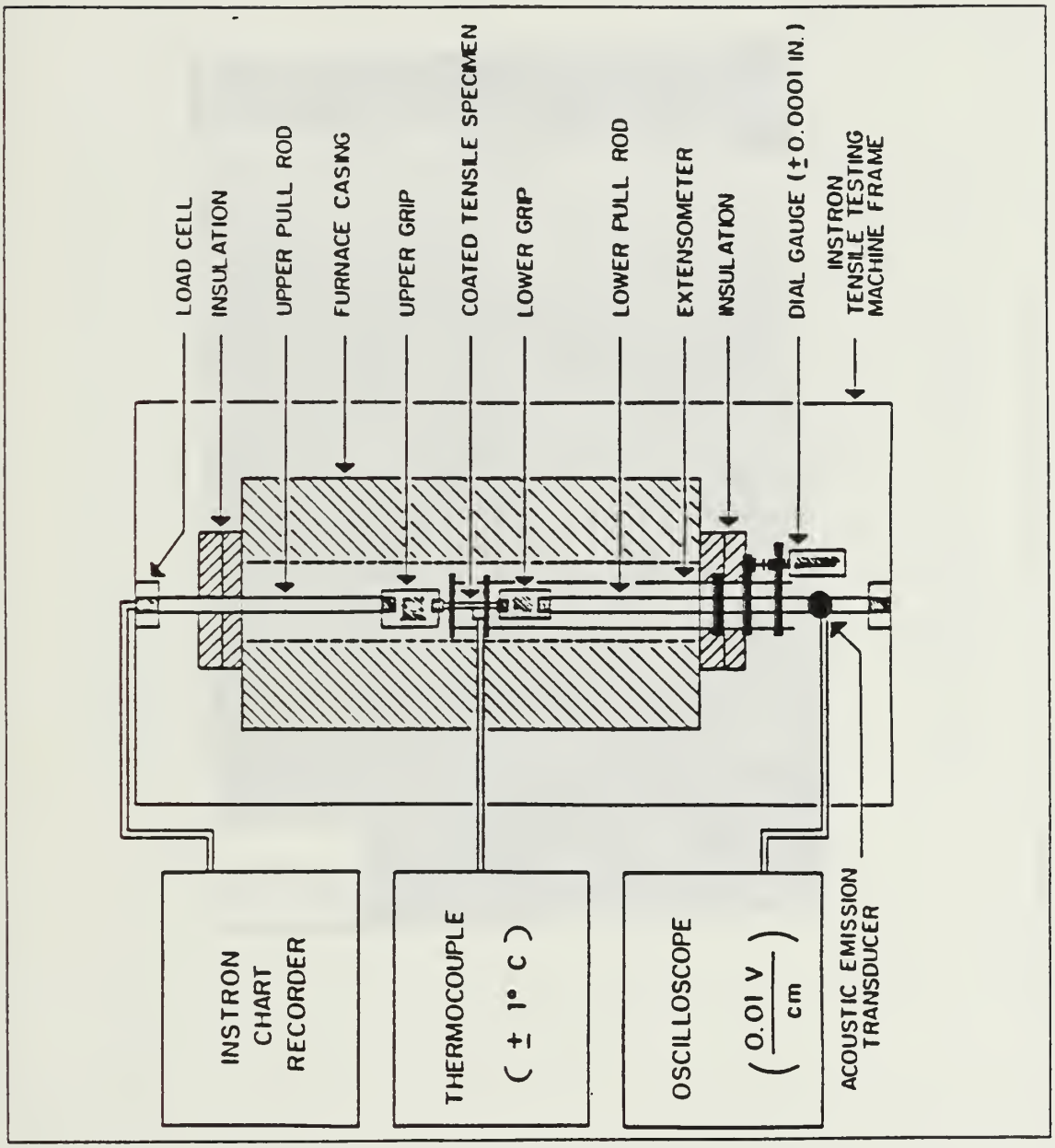

Figure B.1 Experimental Apparatus.

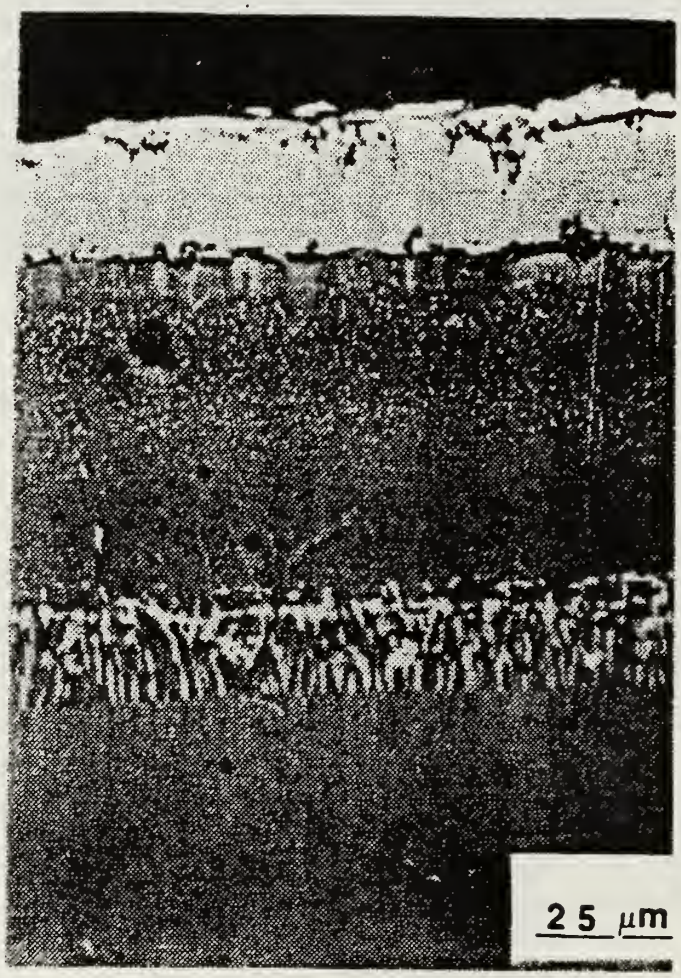

Figure B.2 Coating 1 Microstructure.

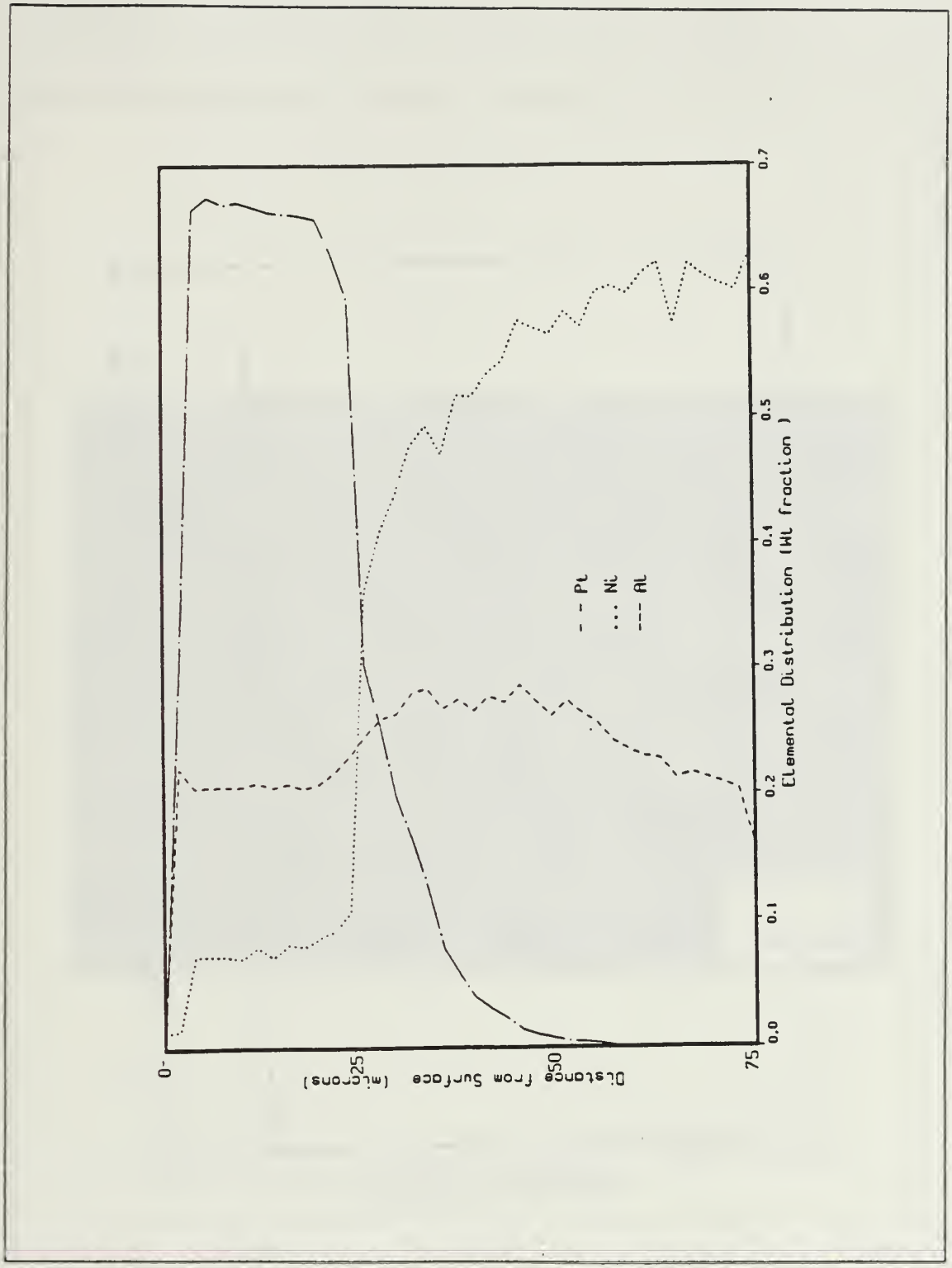

Figure B.3 Coating 1 Elemental Distribution.

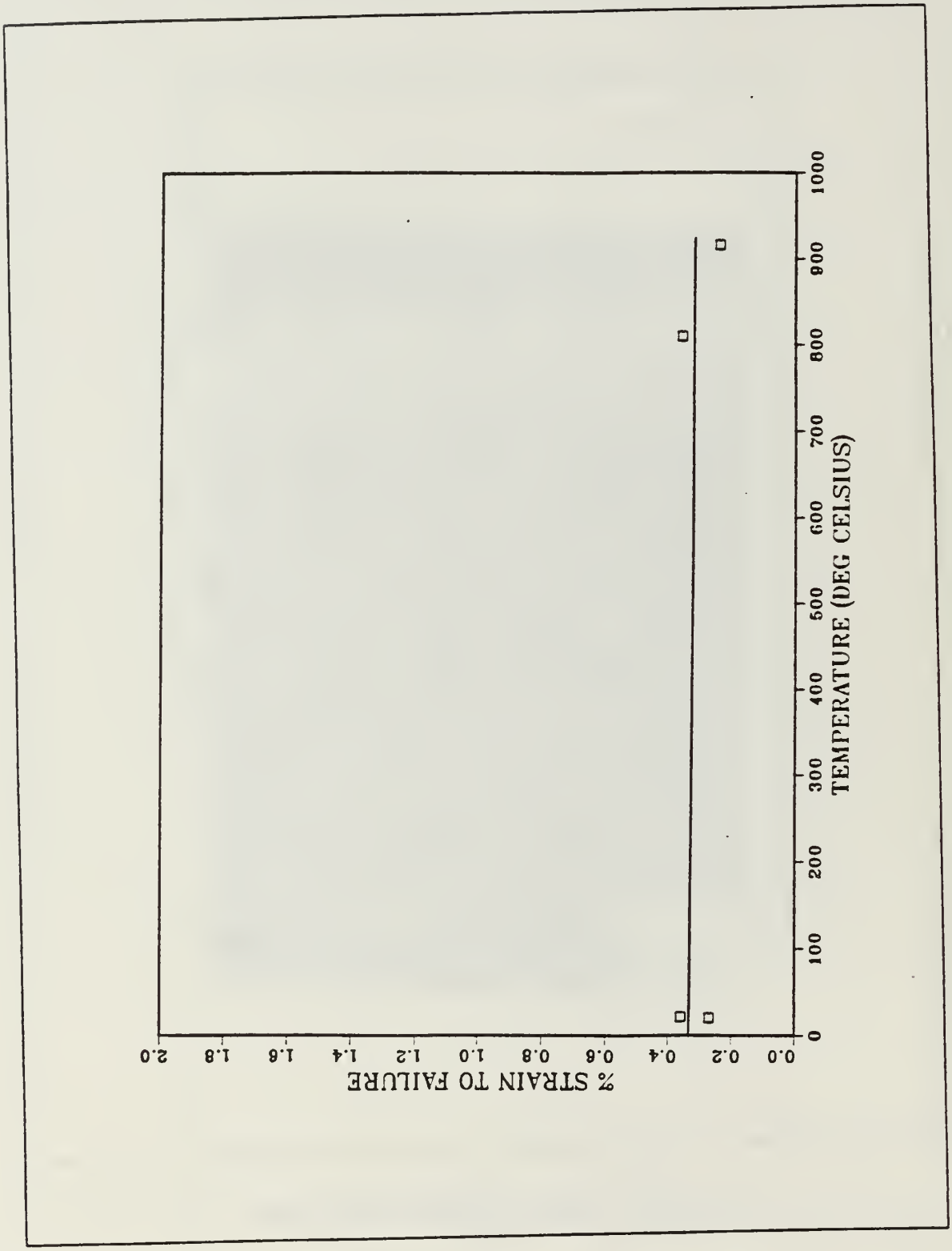

Figure B.4 Coating 1 Strain vs. Temperature.

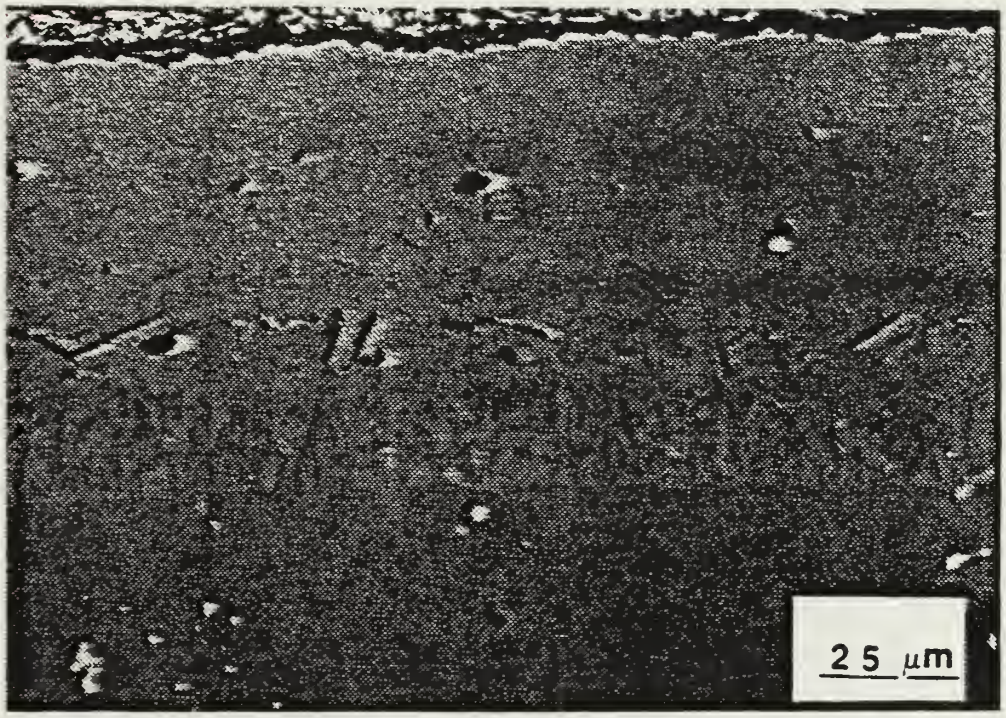

Figure B.5 Coating 2 Microstructure.

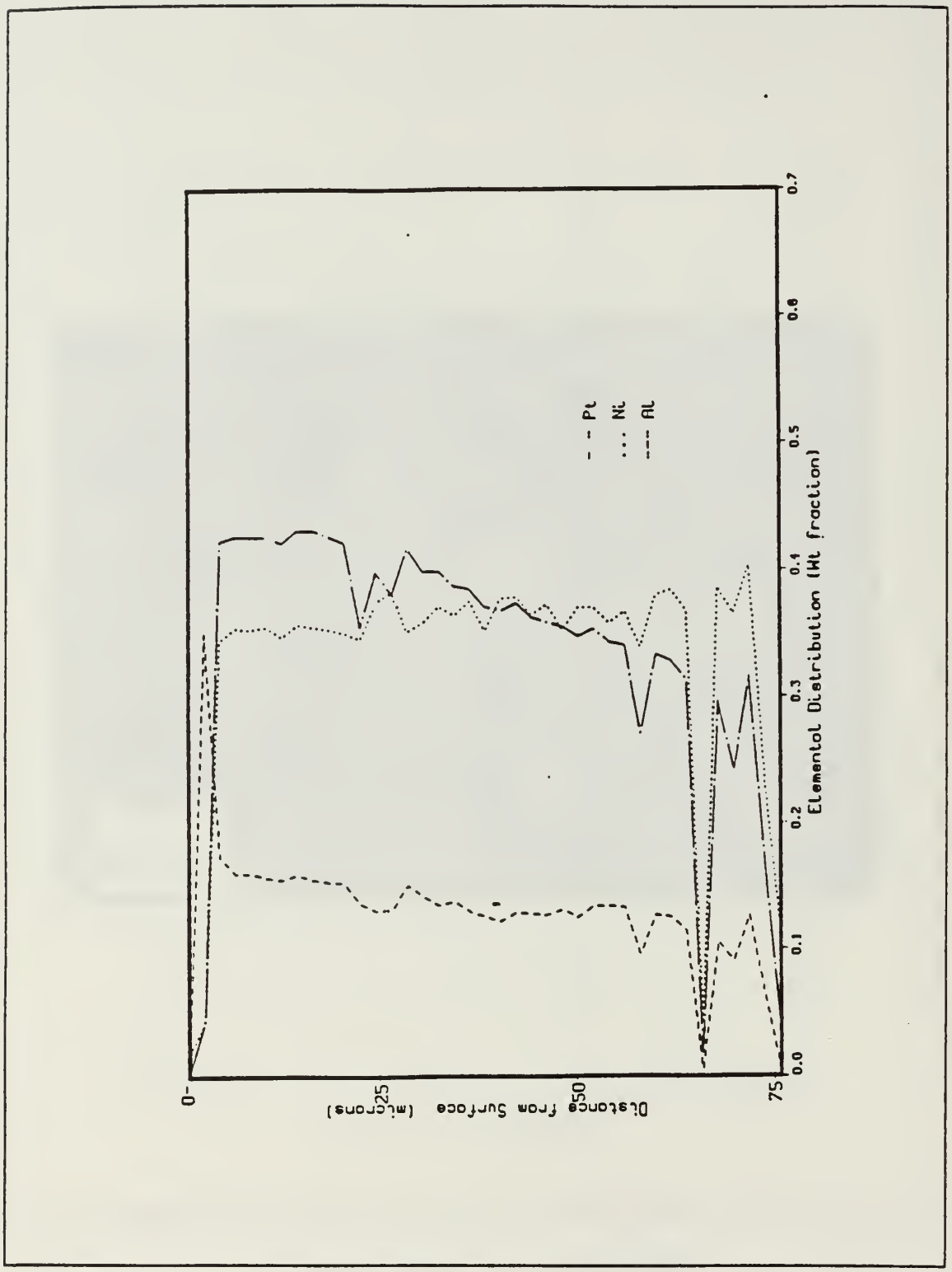

Figure B.6 Coating 2 Elemental Distribution.

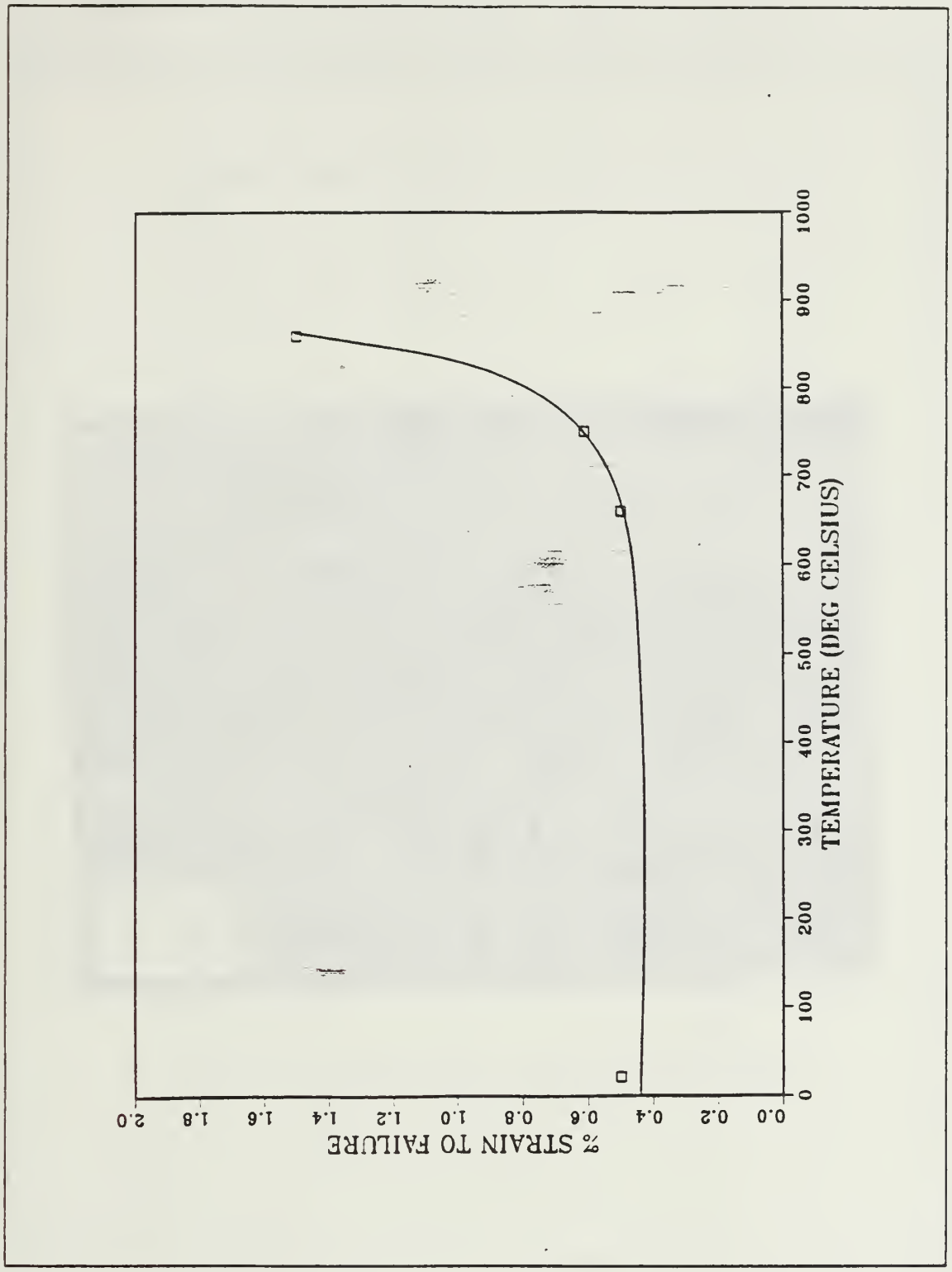

Figure B.7 Coating 2 Strain vs. Temperature.

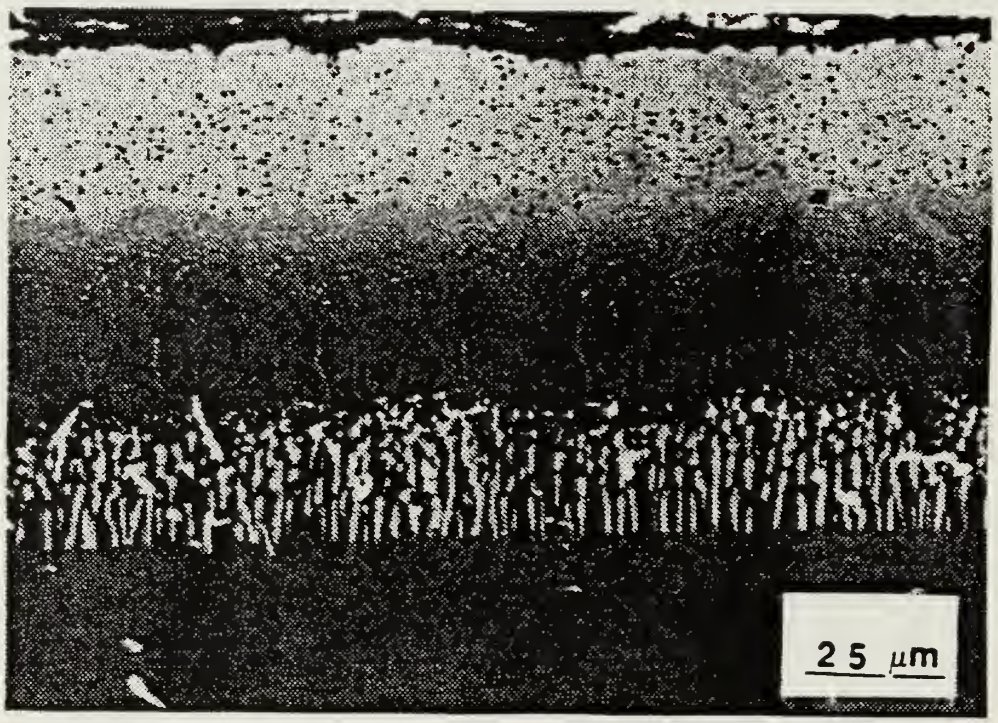

Figure B.8 Coating 3 Microstructure.

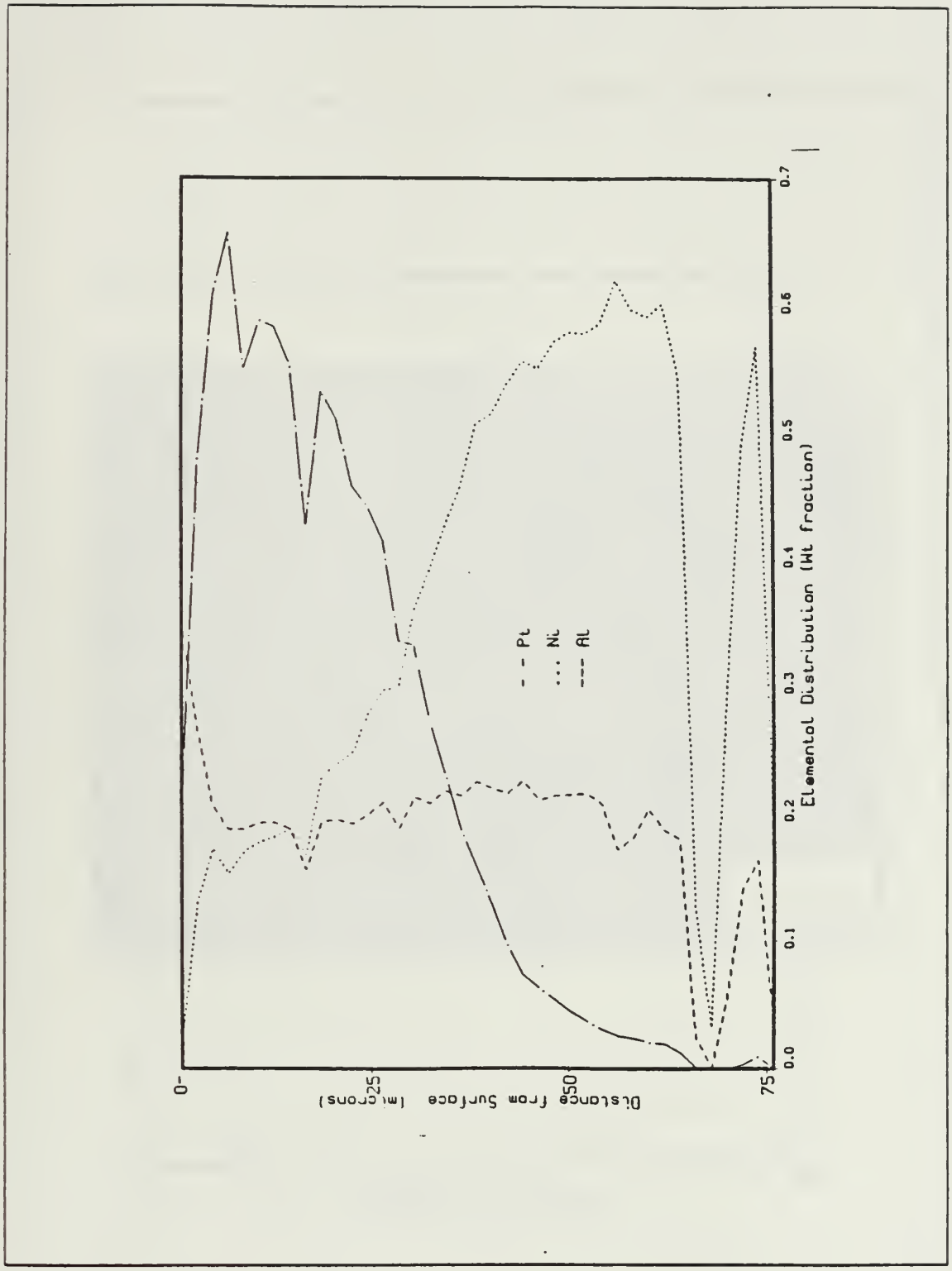

Figure B.9 Coating 3 Elemental Distribution.

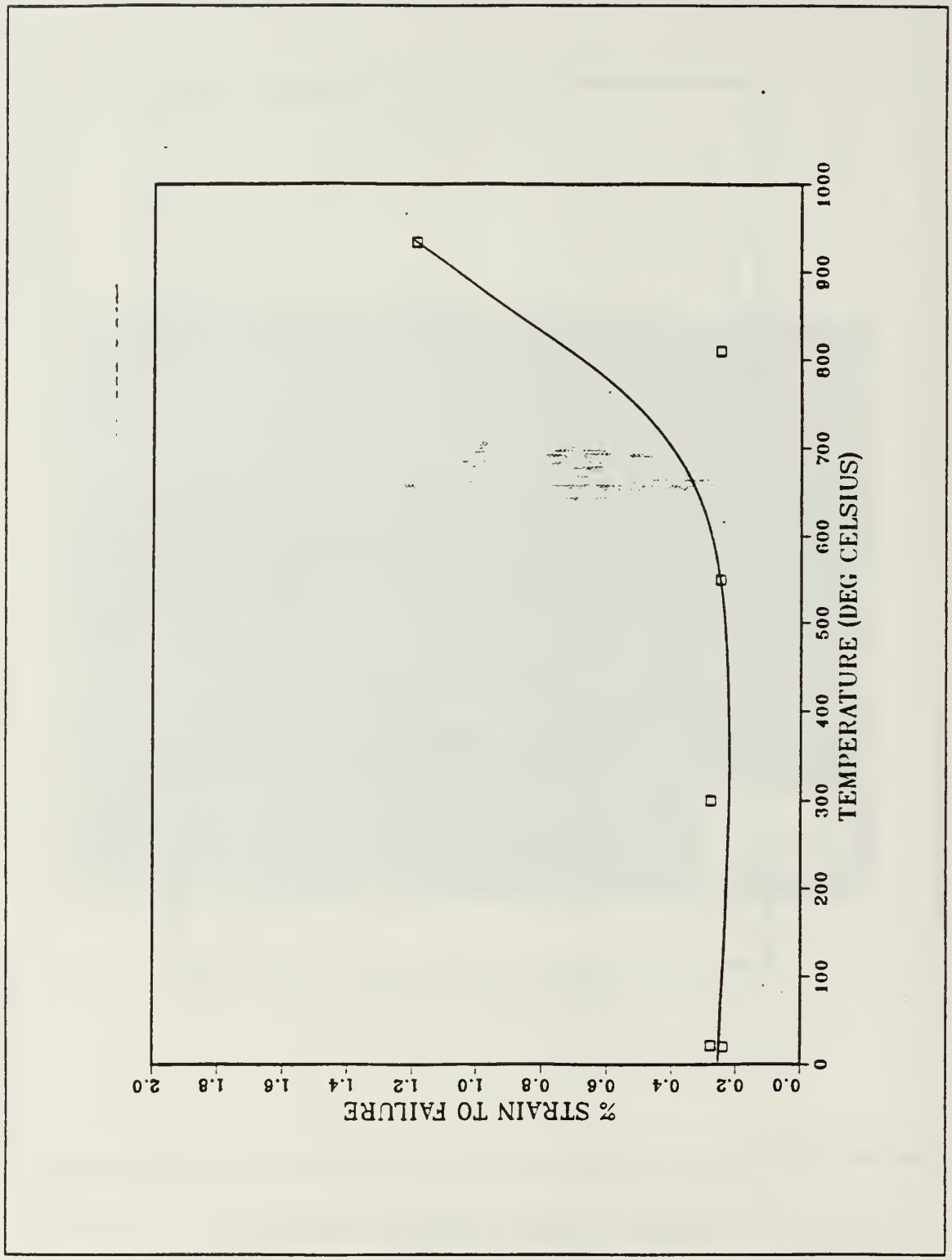

Figure B.10 Coating 3 Strain vs. Temperature.

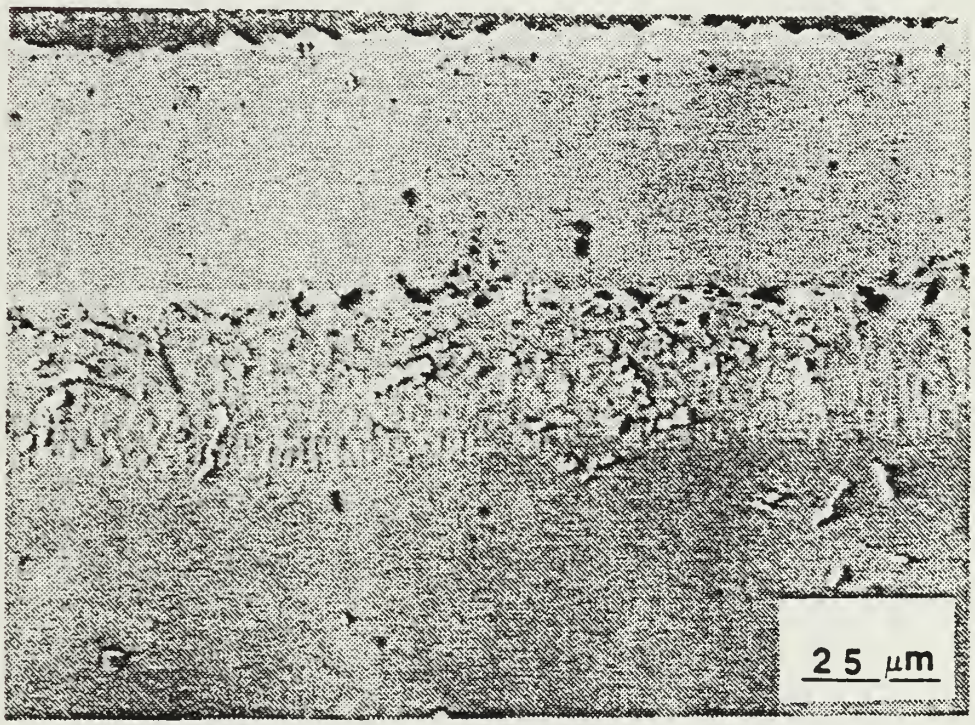

Figure B.11 Coating 4 Microstructure.

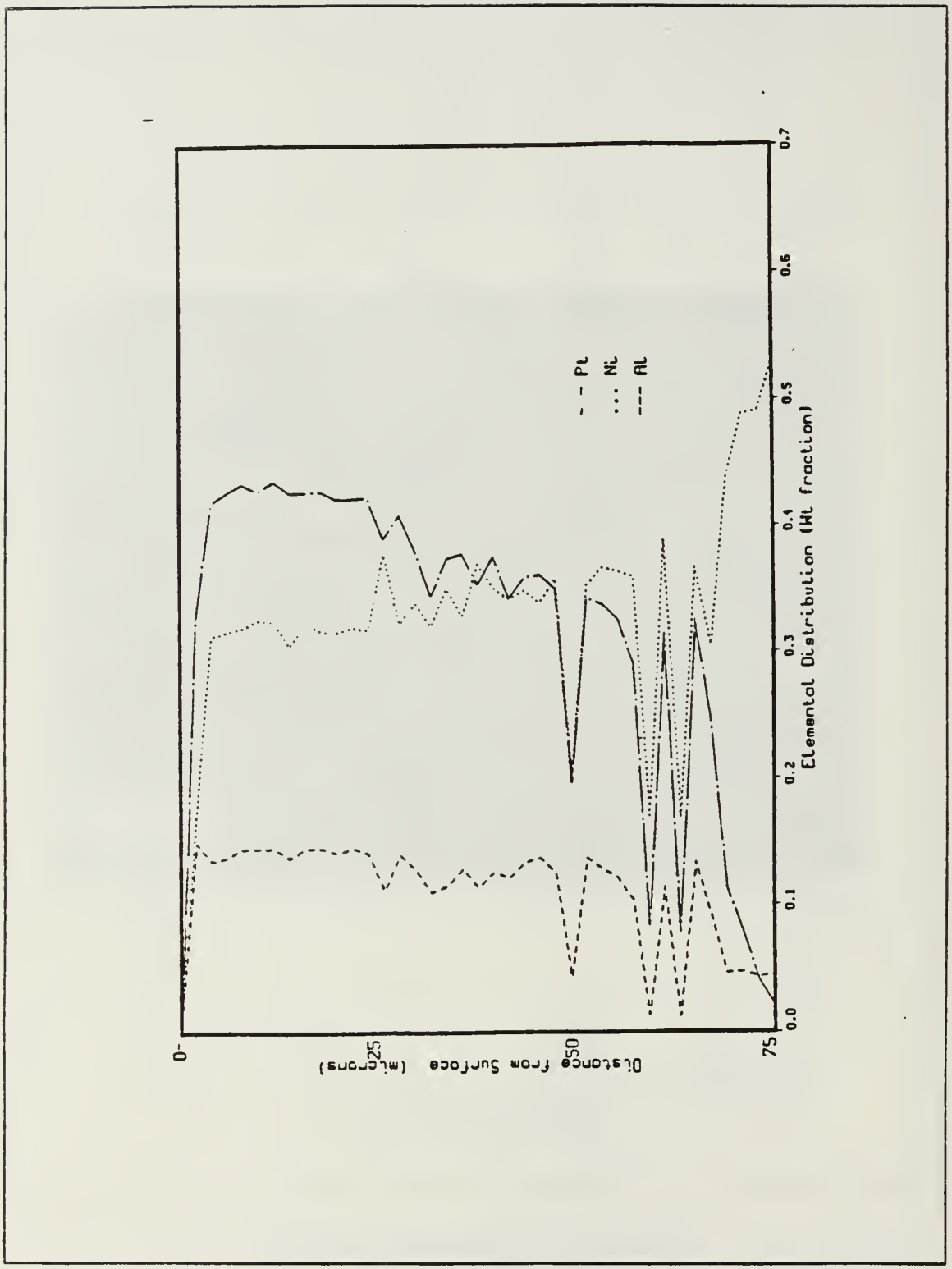

Figure B.12 Coating 4 Elemental Distribution.

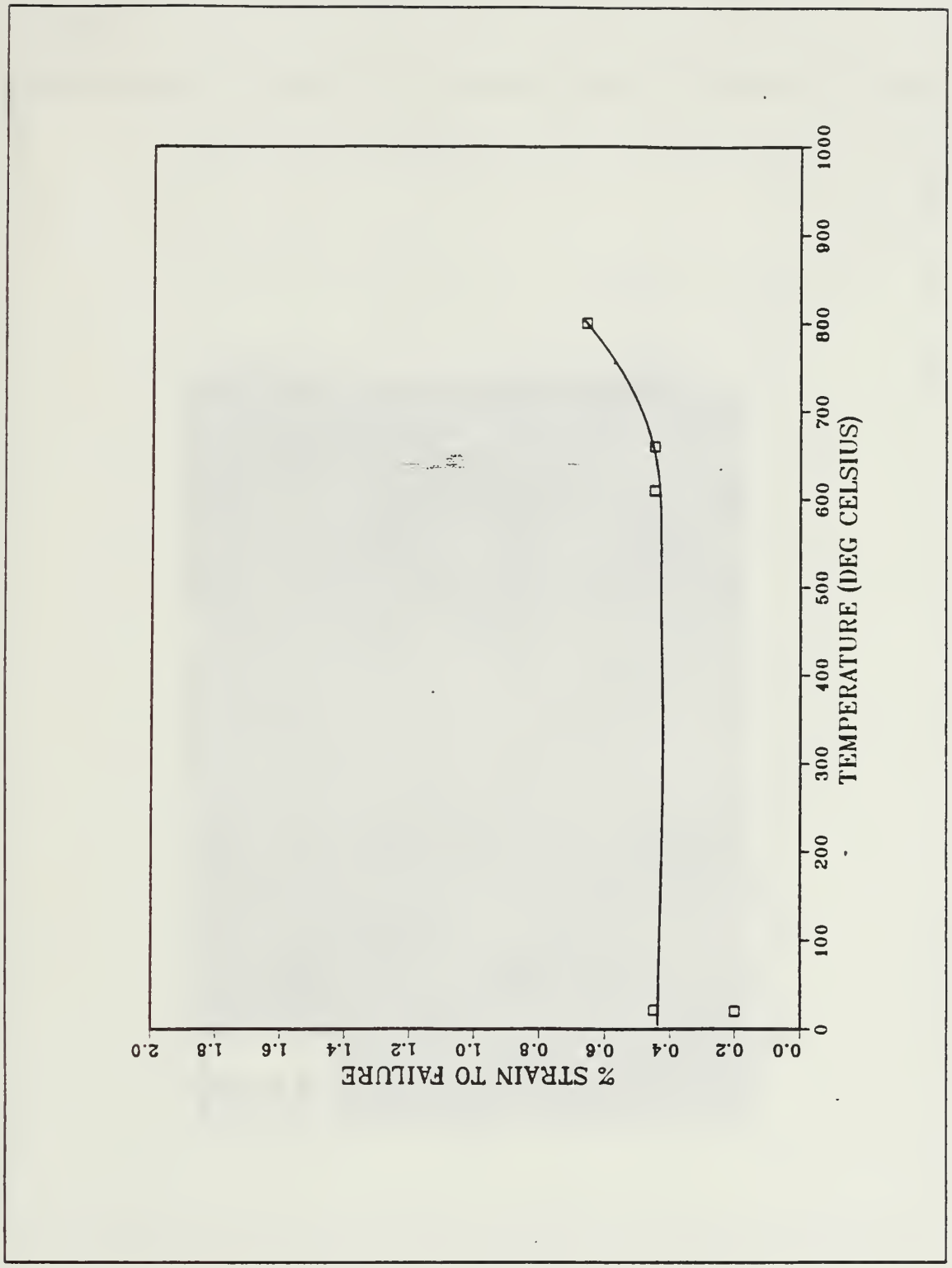

Figure B.13 Coating 4 Strain vs. Temperature.

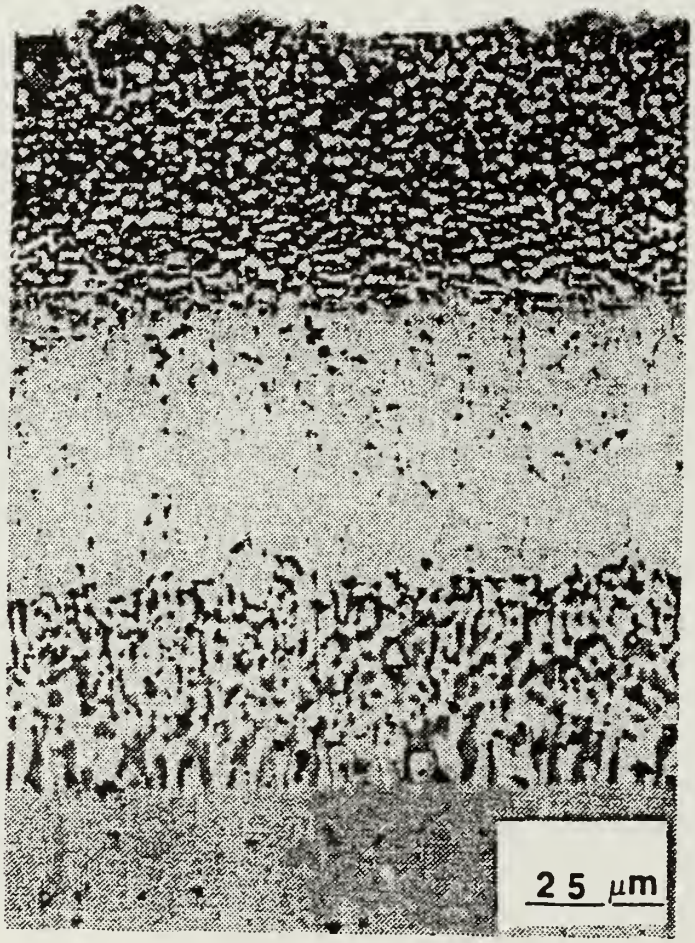

Figure B.14 Coating 5 Microstructure.

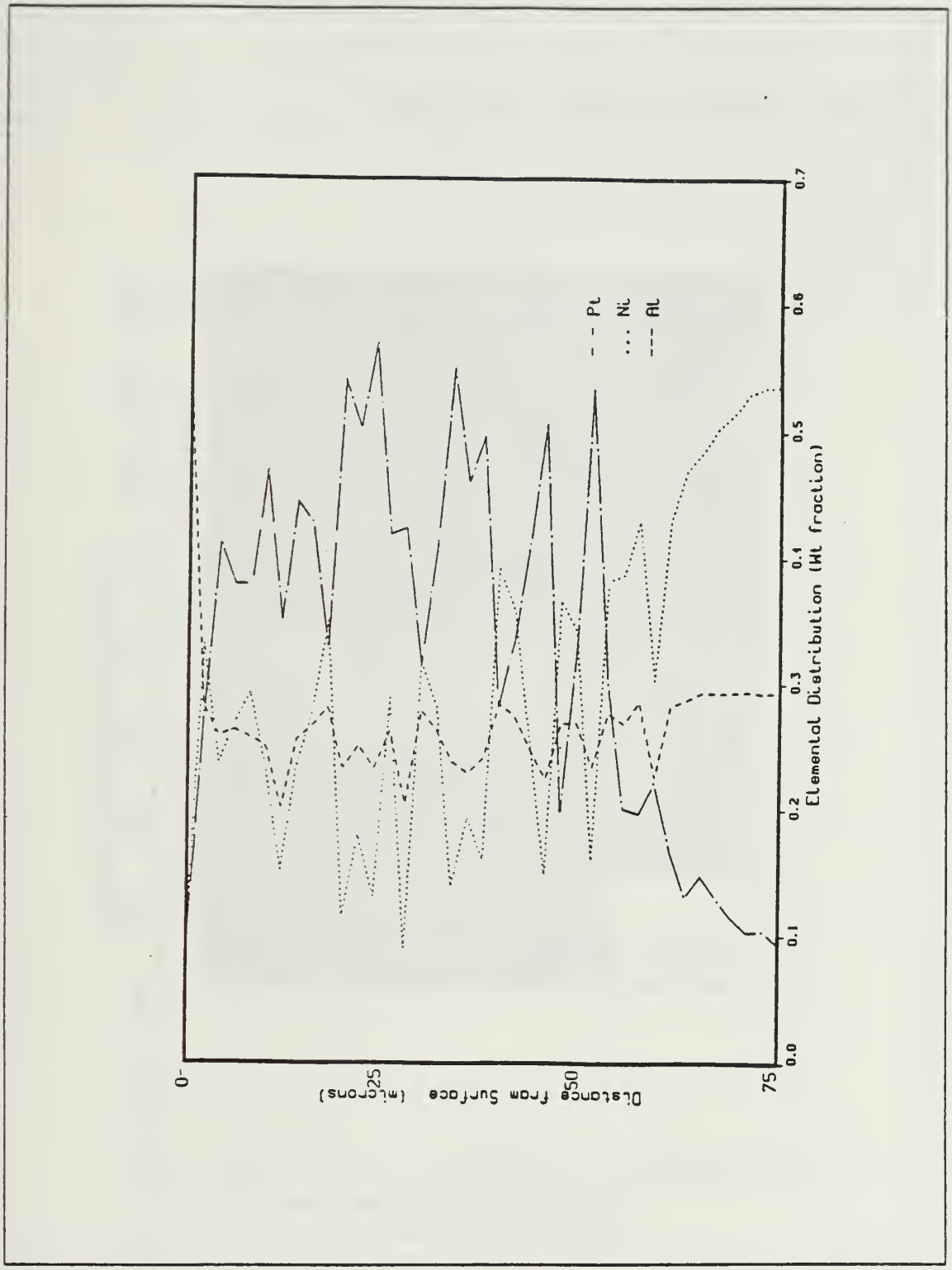

Figure B.15 Coating 5 Elemental Distribution.

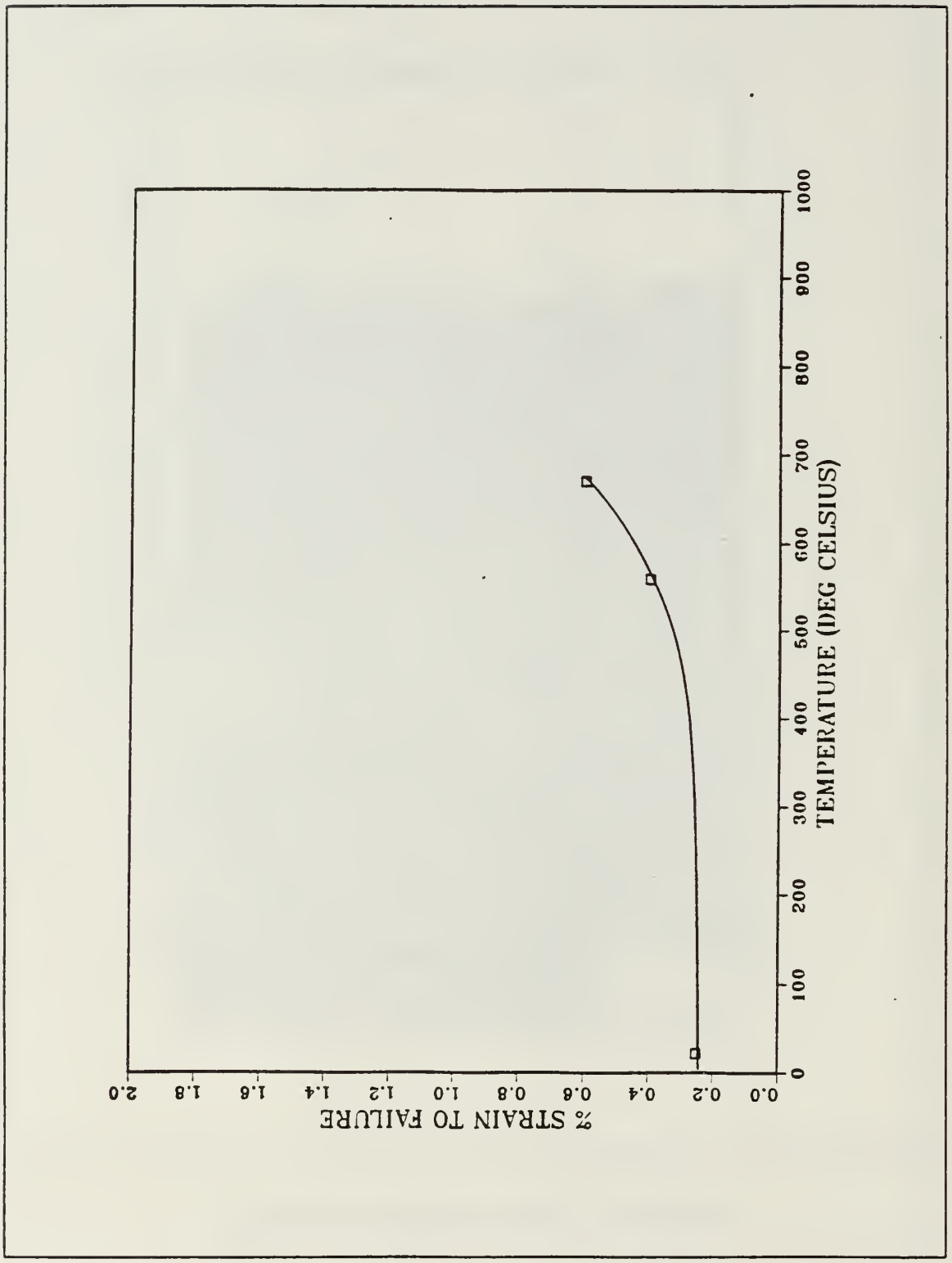

Figure B.16 Coating 5 Strain vs. Temperature.

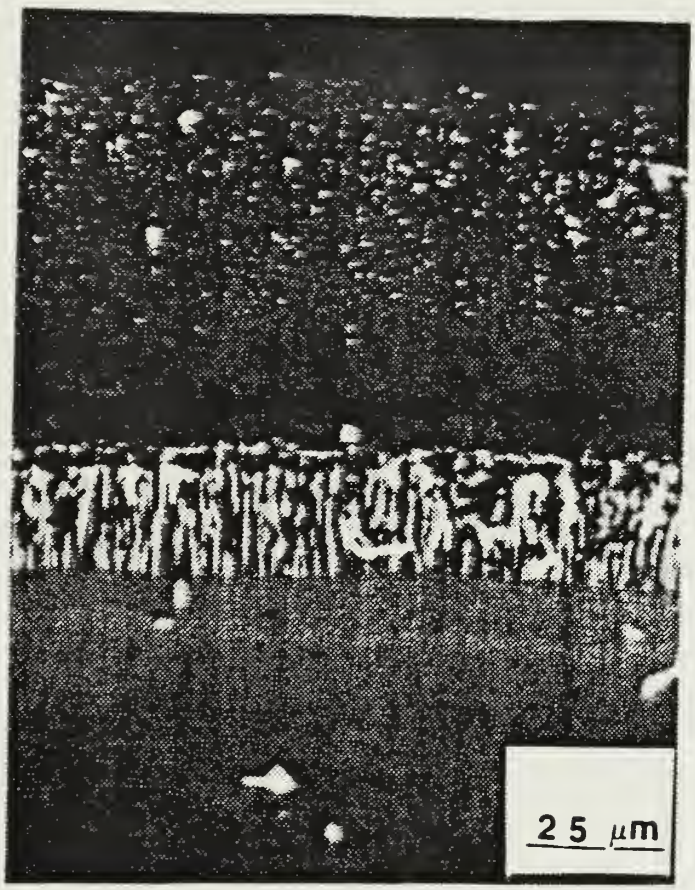

Figure B.17 Coating 6 Microstructure.

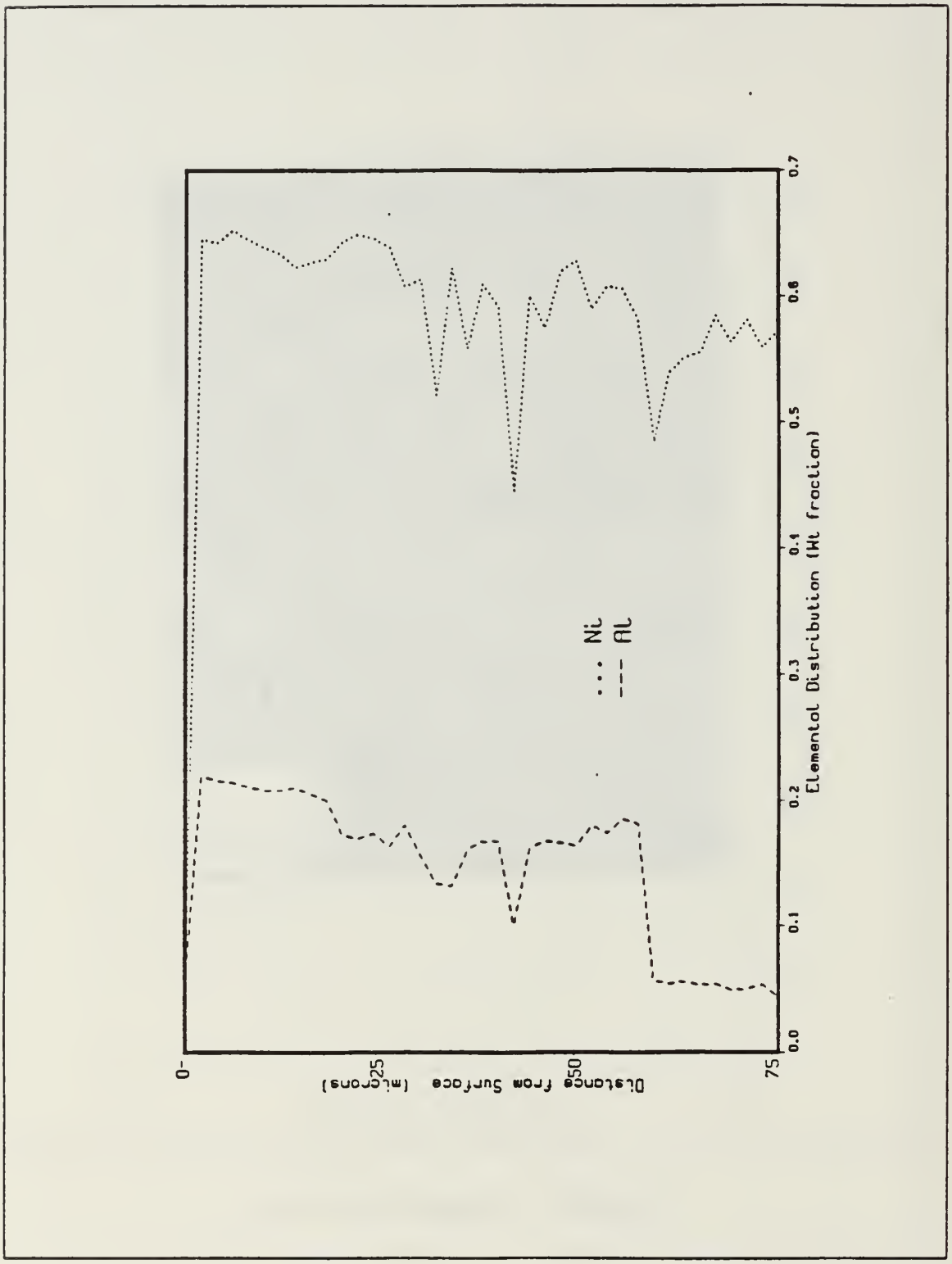

Figure B.18 Coating 6 Elemental Distribution.

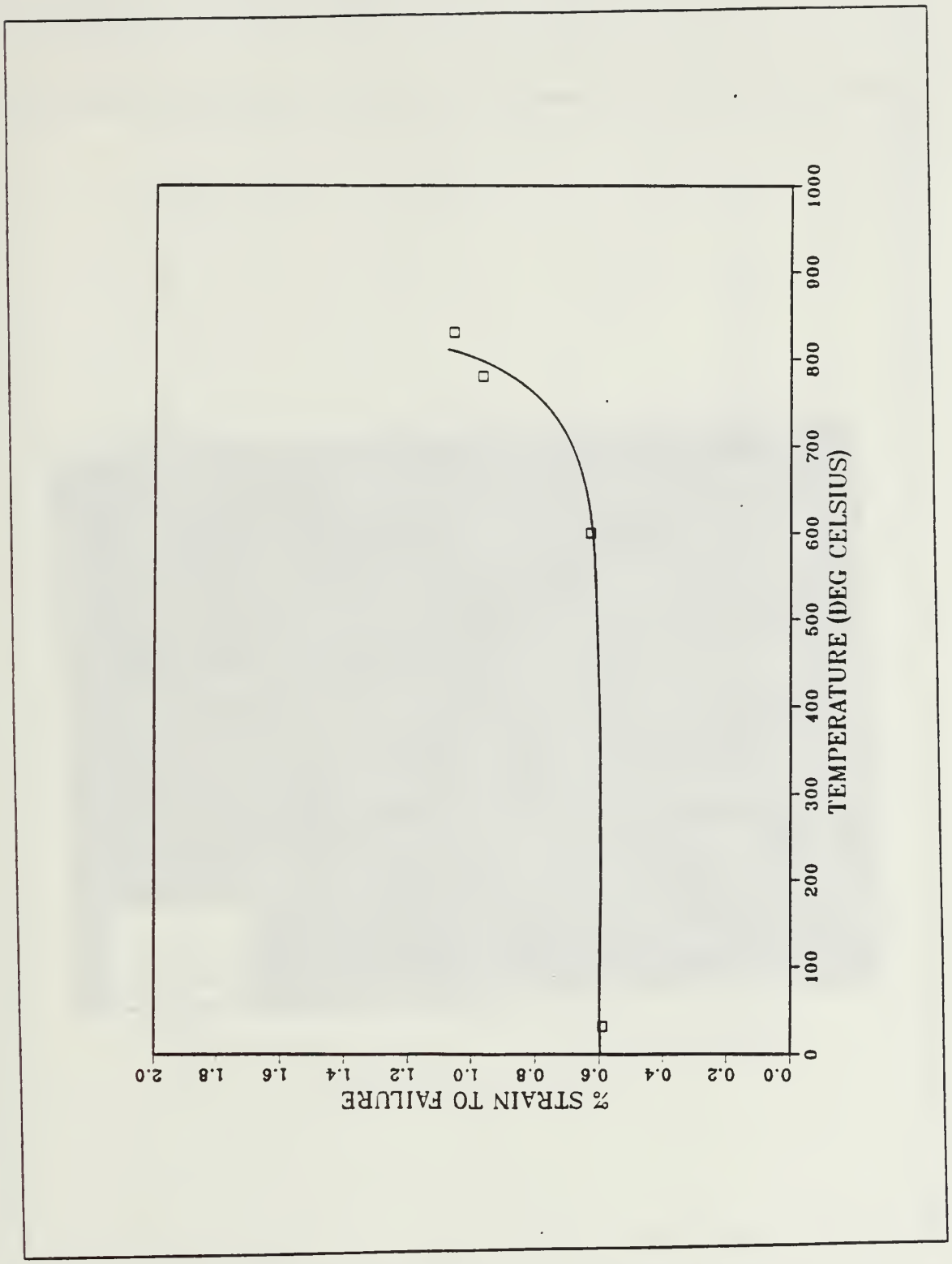

Figure B.19 Coating 6 Strain vs. Temperature.

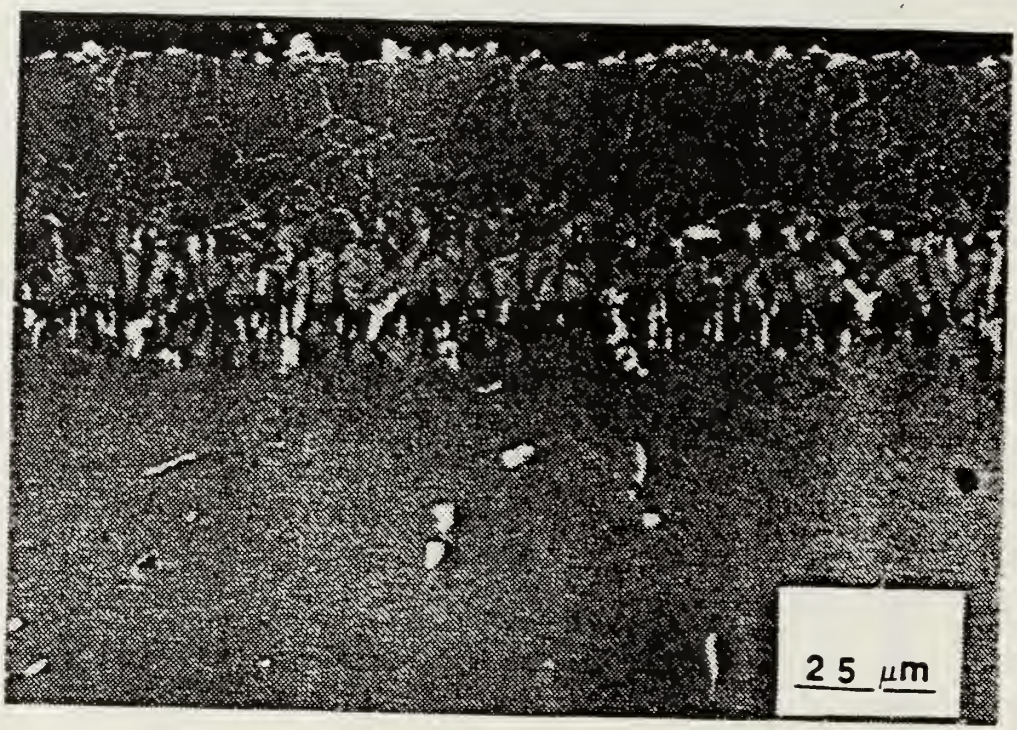

Figure B.20 Coating 7 Microstructure.

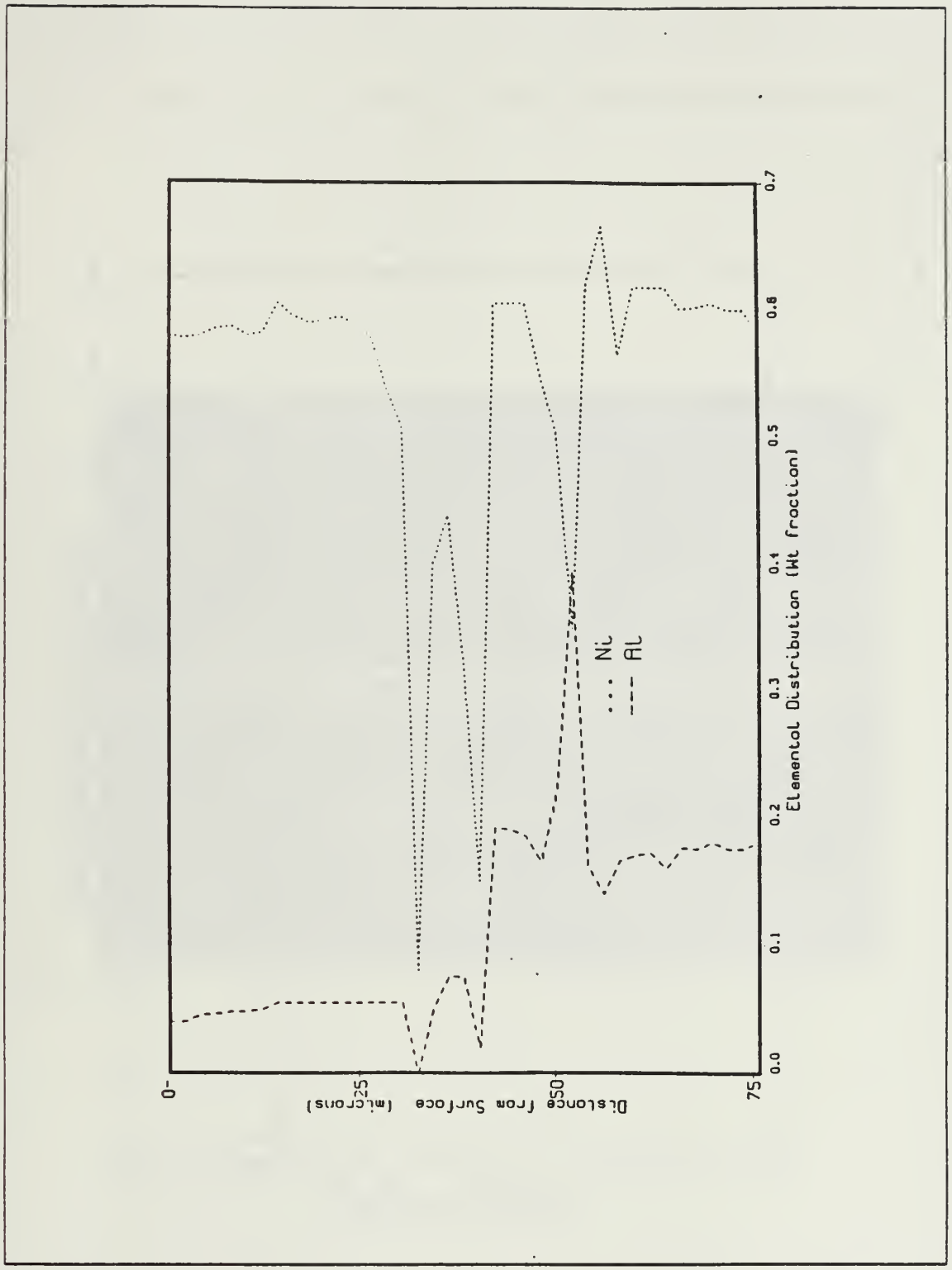

Figure B.21 Coating 7 Elemental Distribution.

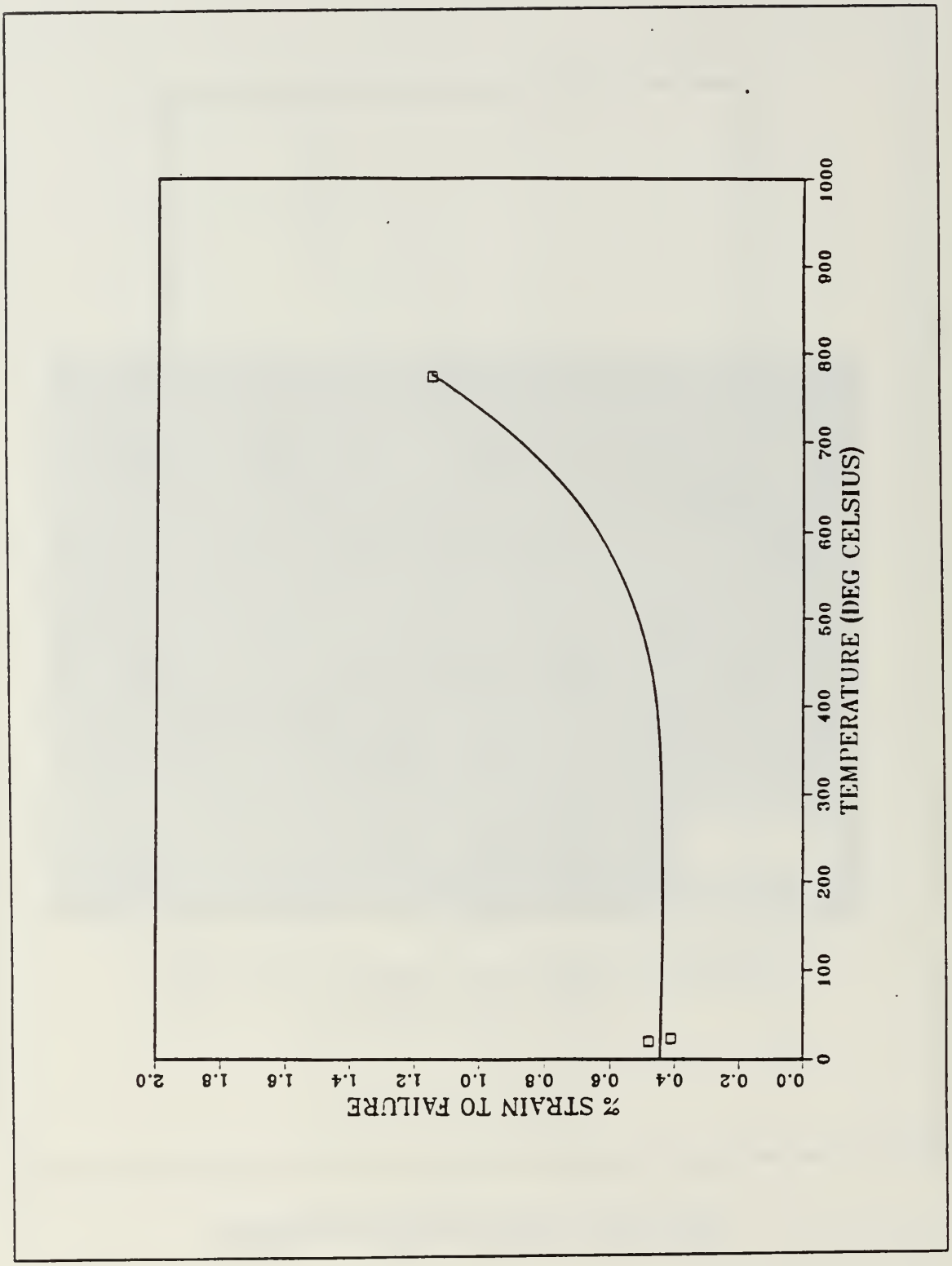

Figure B.22 Coating 7 Strain vs. Temperature.

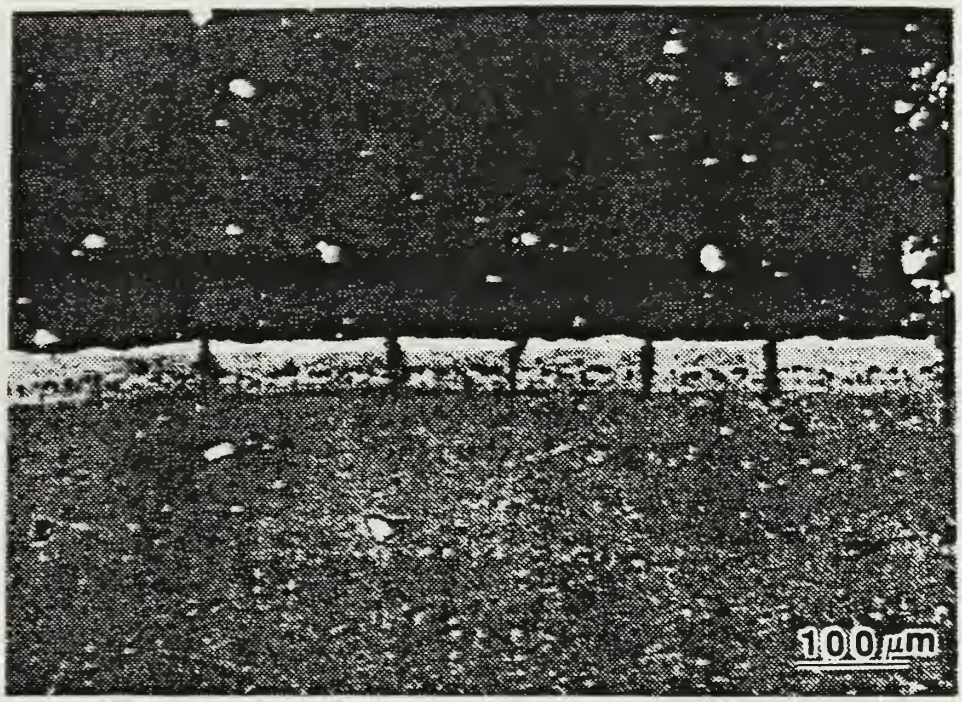

Figure B.23 Typical Cracks at Low Magnification (in section).

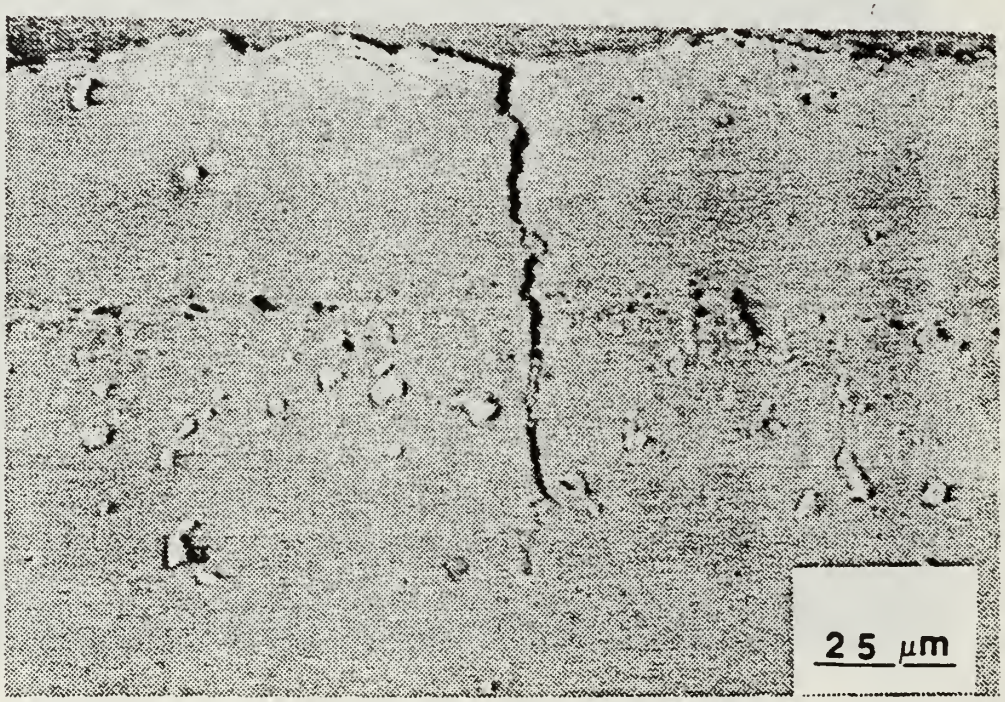

Figure B.24 Typical Crack at High Magnification (in section).

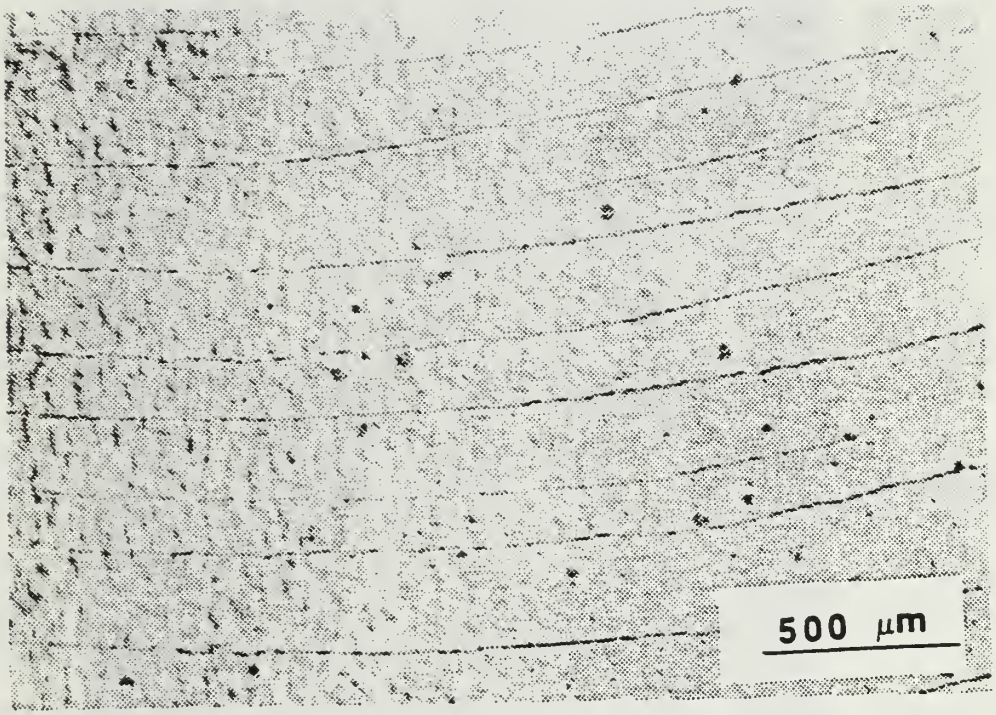

Figure B.25 Typical Cracked Coating Surface.

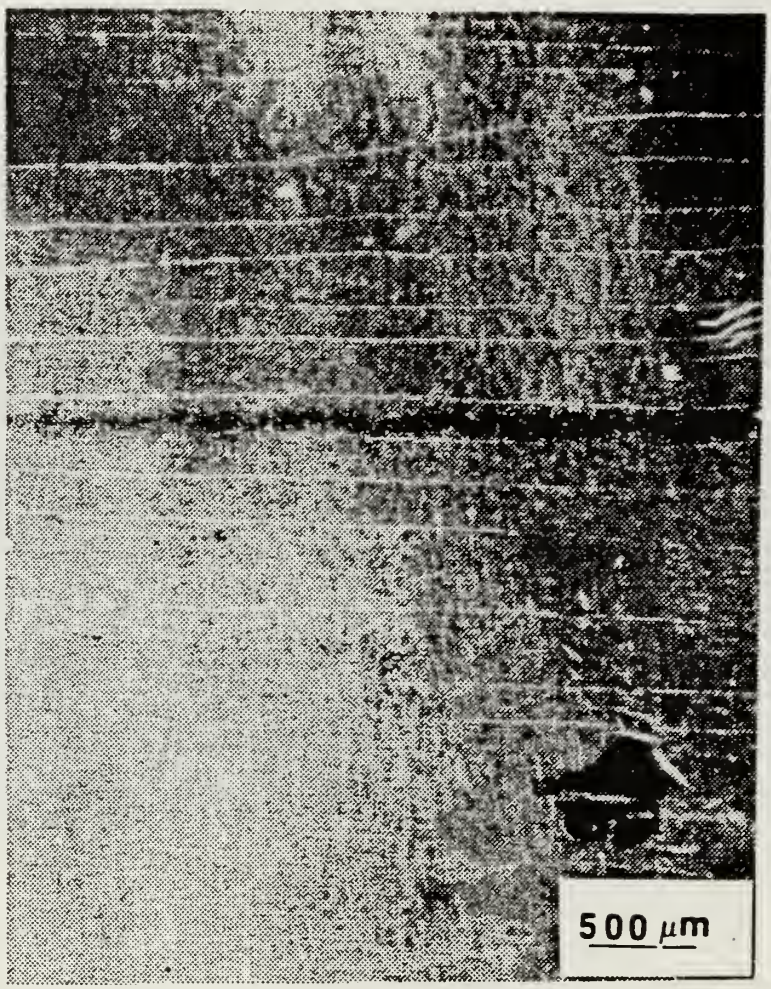

Figure B.26 Replica of Cracked Coating Surface.

LIST OF REFERENCES

1. Wilson, D.G., *The Design of High Efficiency Turbomachinery and Gas Turbines*, MIT Press, 1984.

2. Carleton, R.S, *Qualification of Gas Turbine Engines for U.S. Navy Shipboard Use*, paper presented at Gas Turbine Conference, Washington, D.C., March 17, 1968.

3. Hoppin, G.S., III and Danesi, W., "Manufacturing Processes for Long-Life Gas Turbines," *Journal of Metals*, v. 38, July 1986.

4. Stringer, J. and Whittle, D.P., "High Temperature Corrosion and Coatings of Superalloys," *High Temperature Materials in Gas Turbines*, Elsevier Scientific Publishing Company, 1974.

5. Filby, R.H., Shah, K.R., and Yaghmaie, F., "The Nature of Metals in Petroleum Fuels and Coal - Derived Synfuels," *Ash Deposits and Corrosion Due to Impurities in Combustion Gases*, Hemisphere Publishing Corporation, 1977.

6. Pettit, F.S. and Goward, G.W., "Oxidation-Corrosion-Erosion Mechanisms of Environmental Degradation of High Temperature Materials," *Coatings for High Temperature Applications*, Applied Science Publishers, Ltd, 1983.

7. Smeggil, J.G., Bornstein, N.S., and DeCrescente, M. "The Effect of NaCl(g) on the Na_2SO_4 - Induced Hot Corrosion of NiAl," *Ash Deposits and Corrosion Due to Impurities in Combustion Gases*, Hemisphere Publishing Corporation, 1977.

8. Steinmetz, P., and others, "Hot Corrosion of Aluminide Coatings on Nickel-Base Superalloys," *High Temperature Protective Coatings*, The Metallurgical Society of AIME, 1983.

9. Bornstein, N.S., DeCrescente, M.A., and Roth, H.A., "The Relationship between V_2O_5, Na_2SO_4 and Sulphidation Attack," *Deposition and Corrosion in Gas Turbines*, John Wiley and Sons, 1973.

10. Antolovich, S.D. and Campbell, J.E., "Fracture Properties of Superalloys," *Superalloys Source Book*, American Society for Metals, 1984.

11. American Society for Metals, *Metals Handbook, Desk Edition*, 1985.

12. Versnyder, F.L., "Superalloy Technology - Today and Tomorrow," *High Temperature Alloys for Gas Turbines 1982*, D. Reidel Publishing Company, 1982.

13. Donachie, M.J., Jr., "Introduction to Superalloys," *Superalloys Source Book*, American Society for Metals, 1984.

14. Felix, P.C., "Coating Requirements for Industrial Gas Turbines," *Materials and Coatings to Resist High Temperature Corrosion*, Applied Science Publishers, Ltd, 1978.

15. Betz, W., "Profile of Requirements for Protective Coatings Against High Temperature Corrosion and Some Experience with Their Behavior in Service," *Materials and Coatings to Resist High Temperature Corrosion*, Applied Science Publishers, Ltd, 1978.

16. Meyers, M.A. and Chawla, K.K, *Mechanical Metallurgy*, Prentice Hall, Inc., 1984.

17. Cappelli, P.G., "Coating Processes," *High Temperature Alloys for Gas Turbines*, Applied Science Publishers, Ltd., 1978.

18. Teer, D.G., "Evaporation and Sputter Techniques," *Coatings for High Temperature Applications*, Applied Science Publishers, Ltd., 1983.

19. Steffens, H., "Spray and Detonation Gun Technologies," *Coatings for High Temperature Applications*, Applied Science Publishers, Ltd., 1983.

20. Duret, C. and Pichoir, R., "Protective Coatings For High Temperature Materials: Chemical Vapor Deposition and Pack Cementation Processes," *Coatings for High Temperature Applicaions*, Applied Science Publishers, Ltd., 1983.

21. Strieff, R., Muamba, J.N., and Boone, D.H., "Surface Morphology of Diffusion Aluminide Coatings," paper presented at the International Conference on Metallurgical Coatings, San Diego, California, April 9, 1984.

22. Pichoir, R., "Aluminide Coatings on Nickel or Cobalt-Base Superalloys: Principle Parameters Determining Their Morphology and Composition," *High Temperature Alloys for Gas Turbines*, Applied Science Publishers, Ltd., 1978.

23. Lehnert, G. and Meinhardt, H., "A New Protective Coating for Nickel Alloys," *Electrodeposition and Surface Treatment*, v. 1, 1972.

24. Strieff, R. and Boone, D.H., "The Modified Aluminide Coatings-- Formation Mechanisims of Cr and Pt Modified Coatings," *Reactivity of Solids*, Elsevier Science Publishers, 1985.

25. Dust, M., and others, "Hot Corrosion Resistance of Chromium Modified Platinum-Aluminide Coatings," paper presented at the Gas Turbine Conference, Dusseldorf, West Germany, June 1986.

26. Strieff, R. and Boone, D.H., "Structure of Platinum Modified Aluminide Coatings," paper presented at the NATO Advanced Study Institute on Surface Engineering, Les Arcs, France, July 3, 1983.

27. Hanna, M.D., "The Formation of Platinum Aluminide Coatings on IN 738 and Their Oxidation Resistance," Ph.D. Thesis, Sheffield University, Sheffield, England, 1982.

28. American Society for Testing and Materials, *Standard Methods of Tension Testing of Metallic Materials*, 1983.

29. Telephone conversation between M. Barber, Allison Gas Turbine Company, and Dr. D.H. Boone, Naval Postgraduate School, May 1985.

30. Lehnert, G. and Schmidt, W., "Ductilty of Metallic Diffusion Type Coatings on Nickel-Based Alloys," *Thyssen Edelstahlwerke Ag Forschungsintitut Project 01-ZB-157-D20*, December 1979.

31. Vogel, D.J., *Determination of the Ductile to Brittle Transition Temperature of Platinum-Aluminide Gas Turbine Blade Coatings*, M.S. Thesis, Naval Postgraduate School, Monterey, California, September 1985.

32. Coddet, C., Beranger,G., and Chretien, J.F., "Application fo the Acoustic Emission Technique to the Detection of Oxide Layer Cracking During the Oxidation Process," *Materials and Coatings to Resist High Temperature Corrosion*, 1980.

33. Lowrie, R. and Boone, D.H., "Composite Coatings of CoCrAlY plus Platinum," *Thin Solid Films* v. 45, 1977.

34. Goward, G., "Protective Coatings for High Temperature Alloys: State of Technology," paper presented at the Symposium on Properties of High Temperature Alloys with Emphasis on Environmental Effects, Las Vegas, Nevada, 1976.

INITIAL DISTRIBUTION LIST

		No. Copies
1.	Defense Technical Information Center Cameron Station Alexandria, Virginia 22304-6145	2
2.	Library, Code 0142 Naval Postgraduate School Monterey, California 93943-5002	2
3.	Mr. William Barker Naval Air Development Center Code 60634 Warminster, Pennsylvania 18974-5000	2
4.	Department Chairman, Code 69Mx Department of Mechanical Engineering Naval Postgraduate School Monterey, California 93943-5000	1
5.	Adjunct Professor D.H. Boone, Code 69B1 Department of Mechanical Engineering Naval Postgraduate School Monterey, California 93943-5000	5
6.	Commander, Naval Air Systems Command Department of the Navy (803) Washington, D.C. 20361	1
7.	LCDR L.G. Newman Commander, Naval Logistics Command United States Pacific Fleet CINCPACFLT Box 43 Pearl Harbor, Hawaii 96860-7000	2

220337

Thesis
N4635
c.1

Newman
Structural property effects for platinum modified aluminide coatings.